

GOLDMAN-TURAEV FORMALITY FROM THE KONTSEVITCH INTEGRAL

DROR BAR-NATAN, ZSUZSANNA DANCOS, TAMARA HOGAN, JESSICA LIU,
AND NANCY SCHERICH

ABSTRACT. We present a three dimensional realisation of the Goldman-Turaev Lie bialgebra: we explain how it arises from a low-degree Vassiliev quotient – the *emergent* quotient – of tangles in a thickened punctured disk, modulo a Conway-like relation. Using this characterisation we construct Goldman-Turaev homomorphic expansions (formality isomorphisms) from the Kontsevich integral.

CONTENTS

1. Introduction	2
1.1. Motivation	3
2. Conceptual summary	4
3. Preliminaries: Homomorphic expansions and the Goldman-Turaev Lie bialgebra	8
3.1. Homomorphic expansions and the framed Kontsevich integral	8
3.2. The Goldman-Turaev Lie bialgebra	11
3.3. Associated graded Goldman-Turaev Lie bialgebra	14
4. Expansions for tangles in handlebodies	17
4.1. Framed oriented tangles	17
4.2. Operations on $\tilde{\mathcal{T}}$	19
4.3. The t -filtration on $\tilde{\mathcal{T}}$ and the associated graded $\tilde{\mathcal{A}}$	20
4.4. Operations on $\tilde{\mathcal{A}}$	23
4.5. The s -filtration on $\tilde{\mathcal{T}}$ and $\tilde{\mathcal{A}}$	23
4.6. The Conway quotient	24
5. Identifying the Goldman-Turaev Lie bialgebra	29
5.1. The Goldman Bracket	29
5.2. The Turaev co-bracket	37
6. Glossary of notation	53
References	54

Key words and phrases. knots, links in a handlebody, expansions, finite type invariants, Lie algebras .

1. INTRODUCTION

In 1986, Goldman defined a Lie bracket [Gol86] on the space of homotopy classes of free loops on a compact oriented surface. Shortly after in 1991, Turaev defined a cobracket [Tur91] on the same space¹. This bracket and cobracket make the space of free loops into a Lie bialgebra – known as the Goldman–Turaev Lie bialgebra – which forms the basis for the field of string topology [?] and has been an object of study from many perspectives.

In this paper we, describe a 3-dimensional lift of the Goldman–Turaev Lie bialgebra into a space of tangles in a handlebody. We recover the bracket and cobracket maps as projections of intuitive operations on tangles. We show the Kontsevich integral is homomorphic with respect to these tangle operations. Our main result is informally summarised as follows:

Main Result. *Let $\tilde{\mathcal{T}}$ denote the space of formal linear combinations of tangles in a punctured disc cross an interval $M_p \times I$. Projecting to the bottom $D_p \times 0$, one obtains curves on a punctured disc, and the Goldman–Turaev operations on these curves are induced² by the stacking and flipping operations on the tangles. The Kontsevich integral is a homomorphic expansion for tangles in M_p , and descends to a Goldman–Turaev homomorphic expansion on D_p .*

This result is parallel to Massuyeau’s [Mas18], however, our approach to the cobracket is significantly different and simpler, hence, more likely to give insight into the motivational application described below. Another related result is [?], which constructs Goldman–Turaev expansions from the Khnizhnik–Zamolodchikov connection, a geometric incarnation of the Kontsevich integral.

In more detail, we describe a space $\tilde{\mathcal{T}}$ of formal linear combinations of framed tangles in the handlebody $\mathcal{D}_p \times I$ and operations on this space, which induce the Goldman–Turaev operations in the bottom projection to $D_p \times \{0\}$. The two relevant operations on $\tilde{\mathcal{T}}$ are simple and instinctive tangle operations: the commutator associated to the stacking product, and the difference between a tangle and its vertical flip. Passing to Conway skein quotients of $\tilde{\mathcal{T}}$, defined in Section 4.6, the Goldman bracket arises from this commutator and the Turaev cobracketed from the difference between a tangle and its flip. We study the associated graded spaces and operations, and show that the Kontsevich integral is a homomorphic expansion for these tangles, in other words, intertwines the operations with their associated graded counterparts. We show that therefore, the Kontsevich integral descends to a homomorphic expansion for the Goldman–Turaev Lie bialgebra. For the flipping operation and the Turaev cobracket, the precise statements are subtle, and care needs to be taken with the technical details.

The Conway skein quotients of $\tilde{\mathcal{T}}$ used to recover the Goldman–Turaev Lie Bialgebra arise from “emergent” knots or tangles (See [Kun25] Appendix: Emergent

¹Turaev’s version required factoring out by the constant loop; there is a lift to the full space of homotopy classes of loops, given a framing on the surface [AKKN20].

²In a specific sense defined in Section 2

add referemnces:
chas-sullivan,
kashiwara-vergne, AN,
AT, Formality paper

There are other papers
by Turaev and
Massuyeau–Turaev that
are not mentioned here.

There are also some
references that Yusuke
mentioned that we
should include

I have added a short
discussion on
"emmergent knots" that
is basically of a summary
of the first two
paragraphs Dror’s
appendix. I fell like this
discussion fits nicely here
after we introduce $\tilde{\mathcal{T}}$.
However, this is also
seems like a part of the
motivation and maybe
needs to go in the next
section–however it is not
related to the KV
discussion.

knotted objects). Emergent knots are situated in between homotopy classes of curves (where there is no notion of over or under strands, $\nearrow - \nwarrow = 0$, or $\times = 0$) and classical knots with the usual Reidemeister theory. Emergent knots satisfy a familiar relation in finite type invariant theory $\times \times \times = 0$. More concretely, modding out $\tilde{\mathcal{T}}$ by $\times \times \times = 0$ declares two tangles the same if they differ by two crossing changes. This quotient removes most, but not all, knotted information of the tangles and the slightest of knot theory *emerges*.

1.1. Motivation. The Kashiwara–Vergne equations originally arose from the study of convolutions on Lie groups [?]. The equations were reformulated algebraically in terms of automorphisms of free Lie algebras [?], in this form they are a refinement of the Baker–Campbell–Hausdorff formula for products of exponentials of non-commuting variables.

Kashiwara–Vergne theory has multiple topological interpretations in which Kashiwara–Vergne solutions correspond to certain invariants – called *homomorphic expansions* – of topological objects. The existence of a homomorphic expansion is also called *formality* in the literature, this language is inspired by rational homotopy theory and group theory [?].

One of these topological interpretations is due to the first two authors [BND17], who showed that homomorphic expansions of welded foams – a class of 4-dimensional tangles – are in one to one correspondence with solutions to the KV equations. Recently, a series of papers by Alekseev, Kawazumi, Kuno and Naef [AKKN20, AKKN18b, AKKN18a] drew an analogous connection between KV solutions and homomorphic expansions for the Goldman–Turaev Lie bialgebra for the disc with two punctures (up to non-negligible differences in the technical details). This correspondence was used to generalise the Kashiwara–Vergne equations via considering different surfaces, including those of higher genus.

In other words, there is an intricate algebraic connection between four-dimensional welded foams and the Goldman–Turaev Lie bi-algebra, which strongly suggests that there is a topological connection as well. In addition to the inherent interest in tangles in handlebodies, one goal for this paper is to work towards this connection between the two-dimensional Goldman–Turaev Lie bialgebra and four-dimensional welded foams, by constructing a three-dimensional realisation of the Goldman–Turaev Lie bialgebra, with homomorphic expansions which descend to Goldman–Turaev expansions.

The three-dimensional setting of this paper is motivated from “emergent” knots or tangles (See [Kun25] Appendix: Emergent knotted objects). Emergent knots are situated in between homotopy classes of curves (where there is no notion of over or under strands, $\nearrow - \nwarrow = 0$, or $\times = 0$) and classical knots with the usual Reidemeister theory. Emergent knots satisfy a familiar relation in finite type invariant theory $\times \times \times = 0$. More concretely, modding out $\tilde{\mathcal{T}}$ by $\times \times \times = 0$ declares two tangles the same if they differ by two crossing changes. This quotient removes most, but not all, knotted information of the tangles and the slightest of knot

This is the other spot the emergent knot discussion could go. I have added it here with a different intro sentence

The paper is organised as follows: Section 2 gives a general algebraic framework for how the Goldman–Turaev operations are induced by tangle operations. In Section 3 we give a brief overview of the Kontsevich integral and the Goldman–Turaev Lie bialgebra. In Section 4, we define tangles in handlebodies, relevant operations and Vassiliev filtrations. We identify the associated graded space of tangles as a space of chord diagrams, and introduce the Conway skein quotient. In Section 5, we identify the Goldman–Turaev Lie bialgebra in a low filtration degree, and prove the main theorem.

Acknowledgements. We are grateful to Anton Alekseev, Gwenel Massuyeau, and Yusuke Kuno for fruitful conversations. DBN was supported by NSERC RGPIN 262178 and RGPIN-2018-04350, and by The Chu Family Foundation (NYC). ZD was partially supported by the ARC DECRA DE170101128. NS was supported by the NSF under Grant No. DMS-1929284 while in residence at the Institute for Computational and Experimental Research in Mathematics in Providence, RI, during the Braids Program. We thank the Sydney Mathematical Research Institute and the University of Sydney for their hospitality, and funding for multiple research visits.

sec:conceptsum

We induce the genus zero Goldman-Turaev operations from tangle operations, in the spirit of “connecting homomorphisms”: this Section is a summary of the basic approach. We provide some proofs which are not immediate and use the words *homomorphic expansions*, and *Goldman-Turaev operations* without definition, only mentioning their basic properties which make this conceptual outline coherent; the definitions follow in Section 3.

In the diagram (2.1), the top and bottom rows are exact and the right and left vertical maps are zero, and therefore, by minor diagram chasing, the middle vertical map λ induces a unique map $\eta : C \rightarrow D$, a degenerate case of a connecting homomorphism. In our applications λ is a difference of two maps λ_1 and λ_2 , whose values differ in E but coincide in a quotient F .

eq:inducedconnhom

In Section 5 we present two constructions which produce the Goldman bracket and the Turaev cobracket, respectively, as induced homomorphisms η , from corresponding tangle operations λ_1 and λ_2 . The following example is a schematic version of what will become the argument for the Goldman bracket.

Example 2.1. Let A be an associative algebra, and let $\{L_i\}$ denote the lower central series of A . That is, $L_1 := A$, and $L_{i+1} := [L_i, A]$. Then the L_i are Lie ideals, and let $M_i = AL_i = L_iA$ denote the two-sided ideal generated by L_i . The quotient A/M_1 is the abelianisation of A , denoted by A^{ab} . Then we have the following diagram:

eq:SnakeExample

$$\begin{array}{ccccccc}
 0 & \longrightarrow & K & \longrightarrow & \frac{A}{M_2} \otimes \frac{A}{M_2} & \longrightarrow & A^{ab} \otimes A^{ab} \longrightarrow 0 \\
 & & \downarrow 0 & \nearrow \eta & \downarrow [\cdot, \cdot] & & \downarrow 0 \\
 0 & \longrightarrow & \frac{M_1}{M_2} & \longrightarrow & \frac{A}{M_2} & \longrightarrow & A^{ab} \longrightarrow 0
 \end{array}
 \tag{2.2}$$

Here λ is the algebra commutator, which is indeed the difference between two maps: the multiplication (λ_1) and the multiplication in the opposite order (λ_2). The kernel K of the projection to $A^{ab} \otimes A^{ab}$ is generated by the subalgebras $\left\{ \frac{M_1}{M_2} \otimes \frac{A}{M_2}, \frac{A}{M_2} \otimes \frac{M_1}{M_2} \right\}$ in $\frac{A}{M_2} \otimes \frac{A}{M_2}$. The map η is a well defined commutator map $A^{ab} \otimes A^{ab} \rightarrow \frac{M_1}{M_2}$, given by $\eta(x \otimes y) = [x, y] \bmod M_2$. \square

The goal of this paper is to construct homomorphic expansions (aka formality isomorphisms) for the Goldman-Turaev Lie bialgebra from the Kontsevich integral. In outline, this follows from the naturality property of the construction above, under the associated graded functor, as follows.

Given a short exact sequence

$$0 \longrightarrow A \xrightarrow{\iota} B \xrightarrow{\pi} C \longrightarrow 0,$$

and a descending filtration on B

$$B = B^0 \supseteq B^1 \supseteq B^2 \supseteq \dots \supseteq B^n \supseteq \dots,$$

there is an induced filtration on A given by

$$A = A^0 \supseteq A^1 \supseteq A^2 \supseteq \dots \supseteq A^n \supseteq \dots,$$

where $A^i = \iota^{-1}(\iota A \cap B^i)$. Similarly, there is an induced filtration on C given by

$$C = C^0 \supseteq C^1 \supseteq C^2 \supseteq \dots \supseteq C^n \supseteq \dots$$

where $C^i = \pi(B^n)$.

Lemma 2.2. *If the rows of the diagram (2.1) are exact and filtered so that the filtrations on the left and right are induced from the filtration in the middle, then the induced map η is also filtered.*

Proof. Basic diagram chasing: given $c \in C^n$, since $C^n = \pi(B^n)$, there is a $b \in B^n$ such that $\pi(b) = c$. Since λ is filtered, $\lambda(b) \in E^n$, and $\lambda(b) \in \iota(D)$ by exactness. Since $D^n = \iota^{-1}(\iota(D) \cap E^n)$, we have that $\lambda(b) = \iota(d)$ for a $d \in D^n$. By uniqueness of the induced map, $d = \eta(c)$. \square

The associated graded functor is a functor from the category of filtered algebras (or vector spaces) to the category of graded algebras (or vector spaces). For a filtered algebra

$$A = A^0 \supseteq A^1 \supseteq A^2 \supseteq \cdots \supseteq A^n \supseteq \cdots,$$

the (degree completed) associated graded algebra is defined to be

$$\text{gr } A = \prod_{n=0}^{\infty} A^n / A^{n+1}.$$

The associated graded map of a filtered map is defined in the natural way (as in the proof of Lemma 2.3 below). In general, gr is not an exact functor, but it does preserve exactness for the special class of filtered short exact sequences where the filtrations on A and C are induced from the filtration on B :

lem:ExactGr

Lemma 2.3. *If in the filtered short exact sequence*

$$0 \longrightarrow A \xrightarrow{\iota} B \xrightarrow{\pi} C \longrightarrow 0$$

the filtrations on A and C are induced from the filtration on B , then the associated graded sequence is also exact:

$$0 \longrightarrow \text{gr } A \xrightarrow{\text{gr } \iota} \text{gr } B \xrightarrow{\text{gr } \pi} \text{gr } C \longrightarrow 0.$$

Proof. Since gr is a functor, we know that $\text{gr } \pi \circ \text{gr } \iota = 0$, hence $\text{im } \text{gr } \iota \subseteq \ker \text{gr } \pi$. It remains to show that $\ker \text{gr } \pi \subseteq \text{im } \text{gr } \iota$.

Let $[b] \in B^n / B^{n+1}$, and assume that $\text{gr } \pi([b]) = 0$. Since $\text{gr } \pi([b]) = [\pi(b)] \in C^n / C^{n+1}$, we have $\text{gr } \pi([b]) = 0$ if and only if $\pi(b) \in C^{n+1}$. As the filtration on C is induced from B , we know that $C^{n+1} = \pi(B^{n+1})$. Thus, $\pi(b) \in \pi(B^{n+1})$. Or in other words, there exists $x \in B^{n+1}$ such that $\pi(b) = \pi(x)$. This implies that $\pi(b - x) = 0$ and hence that $b - x \in \iota(A)$ by exactness.

Therefore, $b = x + \iota(a)$ for some $x \in B^{n+1}$ and $a \in A$. It follows that $[b] = [\iota(a)] = \text{gr } \iota([a])$ in B^n / B^{n+1} and hence $\ker \text{gr } \pi \subseteq \text{im } \text{gr } \iota$ as required. \square

gr_induced_is_unique

Corollary 2.4. *If the rows of the diagram in Equation 2.1 are exact, and the filtrations on the left and right are induced from the filtration in the middle, then the rows of the associated graded diagram are also exact, and the unique connecting homomorphism is $\text{gr } \eta$.*

$$(2.3) \quad \begin{array}{ccccccc} 0 & \longrightarrow & \text{gr } A & \longrightarrow & \text{gr } B & \longrightarrow & \text{gr } C \longrightarrow 0 \\ & & \downarrow 0 & & \downarrow \text{gr } \lambda & & \downarrow 0 \\ 0 & \longrightarrow & \text{gr } D & \longrightarrow & \text{gr } E & \longrightarrow & \text{gr } F \longrightarrow 0 \end{array}$$

A dashed curved arrow labeled $\text{gr } \eta$ connects $\text{gr } A$ to $\text{gr } C$ in the top row.

Proof. The exactness of the rows is Lemma 2.3. The induced map is $\text{gr } \eta$ as $\text{gr } \eta$ makes the diagram commute, and the induced map is unique. \square

An expansion for an algebraic structure X is a filtered homomorphism $Z : X \rightarrow \text{gr } X$ (with special properties as explained in Section 3.1). Thus, if expansions exist for each of the spaces A through F , we obtain a multi-cube:

eq:Cube

$$\begin{array}{ccccccc}
 & & A & \xrightarrow{\quad} & B & \xrightarrow{\quad} & C \rightarrow 0 \\
 & \swarrow & \downarrow Z_A & \swarrow \lambda & \downarrow Z_B & \swarrow & \downarrow Z_C \\
 0 \rightarrow & D & \xrightarrow{\quad} & E & \xrightarrow{\quad} & F & \\
 & \downarrow Z_D & & \downarrow Z_E & & \downarrow Z_F & \\
 & \text{gr } D & \xrightarrow{\quad} & \text{gr } E & \xrightarrow{\quad} & \text{gr } F & \rightarrow 0 \\
 & & \swarrow & \swarrow \text{gr } \lambda & \swarrow & \swarrow & \\
 & & \text{gr } A & \xrightarrow{\quad} & \text{gr } B & \xrightarrow{\quad} & \text{gr } C \rightarrow 0
 \end{array}$$

η (top dashed arrow from D to C)
 $\text{gr } \eta$ (bottom dashed arrow from $\text{gr } D$ to $\text{gr } C$)

(2.4)

lem:Naturality

Lemma 2.5. *If, in the multi-cube (2.4) all vertical faces commute, then so does the square:*

eq:HomExp

$$\begin{array}{ccc}
 D & \xleftarrow{\quad \eta \quad} & C \\
 \downarrow Z_D & & \downarrow Z_C \\
 \text{gr } D & \xleftarrow{\quad \text{gr } \eta \quad} & \text{gr } C
 \end{array}$$

(2.5)

Proof. Follows from the uniqueness of the induced maps. \square

In Section 5.1, we will show how the Goldman bracket and Turaev cobracket each arise as induced maps η , where $\lambda = \lambda_1 - \lambda_2$ is a difference of tangle operations. Therefore the Kontsevich integral therefore induces an expansion for the Goldman–Turaev operations, and the commutativity of the square (2.5) for each operation is – by definition – the homomorphicity property of the expansion. This homomorphicity is our main result. The non-trivial vertical face of the multi-cube is the one containing λ , and the commutativity of this for each Goldman–Turaev operation will follow from homomorphicity properties of the Kontsevich integral. Namely, the Kontsevich integral (standing in for Z_B and Z_E) intertwines the appropriate tangle operations λ_0 and λ_1 with their associated graded counterparts. This is the idea behind the approach of this paper.

3. PRELIMINARIES: HOMOMORPHIC EXPANSIONS AND THE GOLDMAN-TURAEV LIE BIALGEBRA

subeseFrmedKms

3.1. Homomorphic expansions and the framed Kontsevich integral. The Kontsevich Integral is the knot theoretic prototype of a *homomorphic expansion*. Homomorphic expansions (a.k.a. formality isomorphisms, well-behaved universal finite type invariants) provide a connection between knot theory and quantum algebra/Lie theory. We begin with a short review of homomorphic expansions from an algebraic perspective, which is outlined – in a slightly different, finitely presentated case – in [BND17, Section 2]. Kontsevich’s original construction gives an invariant of unframed links; for a detailed introduction, we recommend [CDM12, Section 8], or [Kon93, BN95, Dan10]. In this paper we work primarily with framed links and tangles, thus we briefly review the framed versions of the Vassiliev filtration and Kontsevich integral; for more detail see [CDM12, Sections 3.5 and 9.1] and [LM96].

sec:hom_exp

3.1.1. Homomorphic expansions. Let \mathcal{K} denote a given set of knots, links or tangles in \mathbb{R}^3 (e.g., oriented knots), and allow formal linear combinations with coefficients in \mathbb{C} . For links and tangles, allow only linear combinations of embeddings of the same skeleton³. The *Vassiliev filtration* (defined in terms of resolutions of double points $\mathbb{X} = \mathbb{X}^+ - \mathbb{X}^-$) is a decreasing filtration on this linear extension:

$$\mathbb{CK} = \mathcal{K}_0 \supseteq \mathcal{K}_1 \supseteq \mathcal{K}_2 \supseteq \dots$$

The degree completed associated graded space of \mathbb{CK} with respect to the Vassiliev filtration is

$$\mathcal{A} := \prod_{n \geq 0} \mathcal{K}_n / \mathcal{K}_{n+1}.$$

An *expansion* is a filtered linear map $Z : \mathbb{CK} \rightarrow \mathcal{A}$, such that the associated graded map of Z is the identity $\text{gr } Z = \text{id}_{\mathcal{A}}$.

Usually, \mathcal{K} is equipped with additional operations: examples are knot connected sum, tangle composition, strand orientation reversal, etc. Homomorphic expansions are compatible with these operations, and thus allow for a study of \mathcal{K} via the more tractable associated graded spaces.

Specifically, an expansion is *homomorphic* with respect to an operation m , if it intertwines m with its associated graded operation on \mathcal{A} . That is, $Z \circ m = \text{gr } m \circ Z$. A crucial step towards making effective use of this machinery is to get a handle on the space \mathcal{A} in concrete terms: for example, in classical knot theory, \mathcal{A} has a combinatorial description as a space of *chord diagrams* [CDM12, Chapter 4].

There is a natural map ψ from chord diagrams with i chords to $\mathcal{K}_i / \mathcal{K}_{i+1}$, defined by “contracting chords” as in Figure 1. It is not difficult to establish that

³The *skeleton* of a knotted object is the underlying combinatorial object. For example: the skeleton of a link is the number of components; the skeleton of a braid is the underlying permutation; the skeleton of a tangle is the number of strands, connectivity, and number of circle components. In these contexts \mathbb{CK} is a disjoint union of vector spaces, rather than a single vector space.

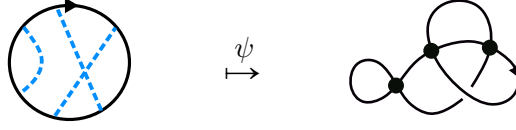


FIGURE 1. Example of ψ mapping a chord diagram to a knot with double points by contracting the chords. The right-hand side represents a well-defined element in $\mathcal{K}_3/\mathcal{K}_4$.

fig:psionchord

ψ is surjective. In the case of classical (oriented, unframed) knots, there are two relations in the kernel of ψ : the 4-Term (4T) and Framing Independence (FI) relations, shown in Figure 2. In fact, these two relations generate the kernel, and ψ descends to an isomorphism on the quotient; this, however, is significantly harder to prove.

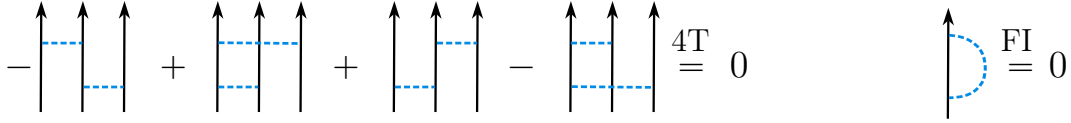


FIGURE 2. The 4T and FI relations, understood as local relations: the strand(s) are part(s) of the skeleton circle, and the skeleton may support additional chords outside the picture shown.

fig:4TFI

The key technique is to construct an expansion as in the following Lemma, [BND17, Proposition 2.7]:

Lemma 3.1. [BND17] *Let \mathbb{CK} be a filtered vector space (or union of vector spaces), and \mathcal{A} the associated graded space of \mathbb{CK} . Let \mathcal{C} be a “candidate model” for \mathcal{A} : a graded linear space equipped with a surjective homogeneous map $\psi : \mathcal{C} \rightarrow \mathcal{A}$. If there exists a filtered map $Z : \mathbb{CK} \rightarrow \mathcal{C}$, such that $\psi \circ \text{gr } Z = \text{id}_{\mathcal{A}}$, then ψ is an isomorphism and $\psi \circ Z$ is an expansion for \mathcal{K} .*

lem:assocgradyoga

$$\begin{array}{ccc}
 \mathbb{CK} & \xrightarrow{Z} & \mathcal{C} \\
 & & \downarrow \psi \\
 & & \mathcal{A}
 \end{array}
 \quad \xRightarrow{\text{gr}} \quad
 \begin{array}{ccc}
 \mathcal{A} & \xrightarrow{\text{gr } Z} & \mathcal{C} \\
 & \searrow \psi \circ \text{gr } Z = \text{id}_{\mathcal{A}} & \downarrow \psi \\
 & & \mathcal{A}
 \end{array}$$

In other words, once one finds a candidate model \mathcal{C} for \mathcal{A} , finding an *expansion valued in \mathcal{C}* also implies that ψ is an isomorphism. In classical Vassiliev theory, \mathcal{K}

is the space of oriented knots, \mathcal{C} is the space of chord diagrams, and a \mathcal{C} -valued expansion is the Kontsevich integral [Kon93].

subsubsec:Framing

3.1.2. Framed theory. In this paper we work with *framed* links and tangles, so we give a brief introduction to the framed version of the general theory summarised in the previous section. For simplicity, we consider links for now.

Let \mathcal{K} denote the set of *framed* links in \mathbb{R}^3 : that is, links along with a non-zero section of the normal bundle. A link diagram is interpreted as a framed link using the blackboard framing. The Reidemeister move R1 move changes the blackboard framing, and by omitting it, one obtains a Reidemeister theory for framed links. In analogy with a double point, a *framing change* is defined to be the difference

$$\uparrow := \uparrow_{\circlearrowleft} - \uparrow.$$

The framed Vassiliev filtration is the descending filtration

$$\tilde{\mathcal{K}} = \tilde{\mathcal{K}}_0 \supseteq \tilde{\mathcal{K}}_1 \supseteq \tilde{\mathcal{K}}_2 \supseteq \dots$$

where $\tilde{\mathcal{K}}_i$ is linearly generated by knots with at least i double points *or framing changes*. The degree completed associated graded space of $\tilde{\mathcal{K}}$ with respect to the framed Vassiliev filtration is

$$\tilde{\mathcal{A}} := \prod_{n \geq 0} \tilde{\mathcal{K}}_n / \tilde{\mathcal{K}}_{n+1}.$$

A natural first guess for a combinatorial description of $\tilde{\mathcal{A}}$ is in terms of chord diagrams with “framing change markings” $\uparrow_{\circlearrowleft}$ on the skeleton, graded by the number of chords and markings. There is a natural surjective graded map $\tilde{\psi}$ from marked chord diagrams onto $\tilde{\mathcal{A}}$, which is contracts chords as in the classical case, and which replaces each marking $\uparrow_{\circlearrowleft}$ with a framing change \uparrow . The kernel of $\tilde{\psi}$ includes the $4T$ relation as before.

In place of the FI relation ($\uparrow_{\circlearrowleft} = 0$), a weaker relation arises from the equality $\uparrow_{\circlearrowleft} - \uparrow_{\circlearrowright} = \uparrow_{\circlearrowleft}$ in $\tilde{\mathcal{K}}$. In fact, $\uparrow_{\circlearrowleft} = \uparrow_{\circlearrowleft} - \uparrow_{\circlearrowright} = (\uparrow_{\circlearrowleft} - \uparrow) + (\uparrow - \uparrow_{\circlearrowright})$, and $\uparrow - \uparrow_{\circlearrowright} = \uparrow_{\circlearrowleft} - \uparrow$ modulo $\tilde{\mathcal{K}}_2$. In other words, the following relation is in the kernel of $\tilde{\psi}$:

$$\uparrow_{\circlearrowleft} = 2 \uparrow_{\circlearrowleft}.$$

Therefore, it is not necessary to have dedicated notation for the framing change markings, since $\uparrow_{\circlearrowleft} = \frac{1}{2} \uparrow_{\circlearrowleft}$. The candidate model for the associated graded space is simply chord diagrams modulo the $4T$ relation, and no FI relation. We denote this space by $\tilde{\mathcal{C}}$.

To show that $\tilde{\psi} : \tilde{\mathcal{C}} \rightarrow \tilde{\mathcal{A}}$ is an isomorphism, it is enough to construct a $\tilde{\mathcal{C}}$ -valued expansion and use Lemma 3.1. This $\tilde{\mathcal{C}}$ -valued expansion is the framed version \tilde{Z} of the Kontsevich integral. For details of this construction see [CDM12, Section 9.1], or [LM96, Gor99].

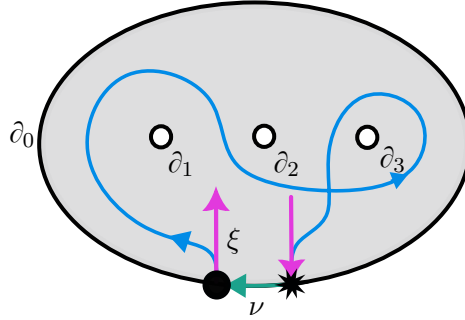


FIGURE 3. D_3 with an immersed loop from \bullet to $*$ with initial tangent vector ξ and terminal tangent vector $-\xi$. The path along the boundary from $*$ to \bullet is ν .

fig:DP

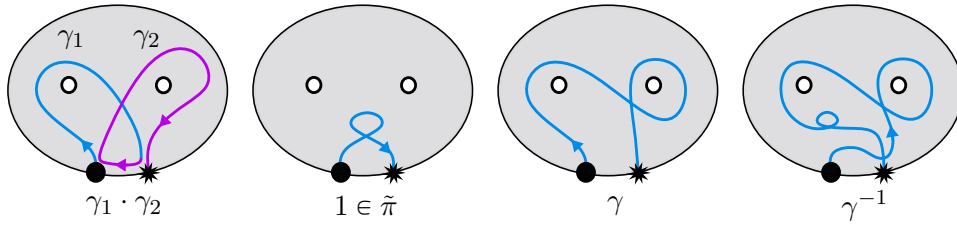


FIGURE 4. The group structure on $\tilde{\pi}$.

fig:DPGroup

subsec:IntroGT

3.2. The Goldman-Turaev Lie bialgebra. In order to define the Goldman-Turaev Lie bialgebra, we need to recall some basic definitions and notation.

Let D_p denote p -punctured disc, with $p+1$ circle boundary components $\partial_0, \partial_1, \dots, \partial_p$, embedded in the complex plane so that ∂_0 is the outer boundary, as in Figure 3. In particular, the plane-embedding specifies a framing (trivialisation of the tangent bundle) on D_p , and thus immersed loops in D_p are equipped with a notion of *rotation number*.

Let $\pi = \pi_1(D_p, *)$ denote the fundamental group of D_p with basepoint $* \in \partial_0$. We denote by $\mathbb{C}\pi$ the group algebra of π .

We also need to consider based paths. Let \bullet and $*$ be two “nearby” basepoints on ∂_0 and ξ be the direction of the inward pointing normal vector to ∂_0 at \bullet and $*$. Let $\tilde{\pi} = \tilde{\pi}_{\bullet,*}$ denote the set of regular homotopy classes of immersed curves $\gamma : ([0, 1], 0, 1) \rightarrow (D_p, \bullet, *)$, so that $\dot{\gamma}(0) = \xi$, and $\dot{\gamma}(1) = -\xi$, as shown in Figure 3. Note that the rotation number is invariant under regular homotopy. Recall that $\tilde{\pi}$ is in fact a group, illustrated in Figure 4 and defined as follows:

- (1) Let ν denote the path from $*$ to \bullet along ∂_0 . The group product $\gamma_1 \cdot \gamma_2$ is the smooth concatenation of γ_1 with ν followed by γ_2 .

- (2) The group identity is the class of paths which, when composed with ν , become contractible loops of rotation number zero.
- (3) The inverse of γ is the concatenation $\overline{\nu} \overline{\gamma} \nu^*$ where the overline denotes the reverse path, and ν^* includes a negative twist (to ensure that the rotation number of $\gamma \cdot \gamma^{-1}$ is 0). The beginning and end of the path is adjusted in an epsilon neighbourhood of the base points to have inward and outward pointing tangent vectors, as in Figure 4.

Denote by $\mathbb{C}\tilde{\pi}$ the group algebra of $\tilde{\pi}$. There is a forgetful map $\tilde{\pi} \rightarrow \pi$ which maps γ to the (non-regular) homotopy class of $\gamma\nu$. This linearly extends to a forgetful map $\mathbb{C}\tilde{\pi} \rightarrow \mathbb{C}\pi$.

For an algebra A we denote by $|A|$ the *linear*⁴ quotient $A/[A, A]$, where $[A, A]$ denotes the subspace spanned by commutators $[x, y] = xy - yx$ for $x, y \in A$. We denote the quotient (trace) map by $|\cdot| : A \rightarrow |A|$. In our context, $|\mathbb{C}\pi|$ has an explicit description as the \mathbb{C} -vector space generated by homotopy classes of free loops in D_p . In a similar but more subtle fashion, $|\mathbb{C}\tilde{\pi}|$ is spanned by *regular* homotopy classes of immersed free loops, where $|\gamma|$ denotes the class of $\gamma\nu$ as a free immersed loop.

The Goldman–Turaev Lie bialgebra comes in two flavours: *original* and *enhanced*. The original construction of the Goldman bracket is a Lie bracket on $|\mathbb{C}\pi|$. However, the original Turaev cobracket is only well-defined on $|\mathbb{C}\pi| = |\mathbb{C}\pi|/\mathbb{C}\mathbf{1}$, the linear quotient by the homotopy class of the constant loop. The space $|\mathbb{C}\pi|$ is a Lie bialgebra with this cobracket and the Goldman bracket, which descends from $|\mathbb{C}\pi|$. There is an enhancement [AKKN18b] of the cobracket, which promotes it to $|\mathbb{C}\pi|$, thereby making $|\mathbb{C}\pi|$ a Lie bialgebra under the Goldman bracket and the enhanced cobracket. In [AKKN18b] this enhancement is necessary in order to establish the relationship between the Goldman–Turaev Lie bialgebra and Kashiwara–Vergne theory. To define the enhanced cobracket, a curve in $|\mathbb{C}\pi|$ is lifted to an immersed curve with a fixed rotation number. Below we review the definitions of the Goldman bracket and the enhanced version of the Turaev cobracket.

The Goldman Bracket sums over smoothing intersections between two free loops. For a free loop α in $|\mathbb{C}\pi|$ and a point q on α , denote by α_q the loop α based at q .

def:bracket

Definition 3.2 (The Goldman bracket). Let $\alpha, \beta \in |\mathbb{C}\pi|$ be free loops with homotopy representatives chosen so that there are only finitely many transverse double intersections between α and β . The Goldman bracket $[\cdot, \cdot]_G : |\mathbb{C}\pi| \otimes |\mathbb{C}\pi| \rightarrow |\mathbb{C}\pi|$ is given by

$$[\alpha, \beta]_G := - \sum_{q \in \alpha \cap \beta} \varepsilon_q |\alpha_q \beta_q|,$$

⁴Not to be confused with the abelianisation of A . In particular, $|A|$ does not inherit an algebra structure from A .

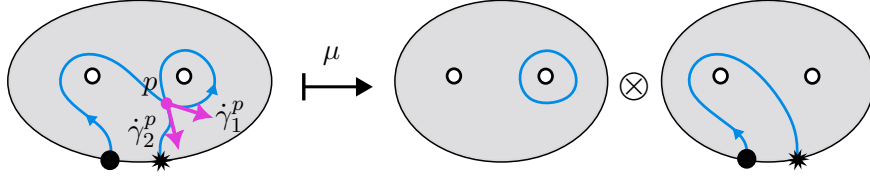


fig:defmu

FIGURE 5. Example of the self intersection map μ where $\epsilon_p = -1$.

where $\epsilon_q = \epsilon(\dot{\alpha}_q, \dot{\beta}_q) \in \{\pm 1\}$ is the local intersection number of α and β at q , $\alpha_q \beta_q$ is the concatenation of α_q and β_q , and the extension to $|\mathbb{C}\pi|$ is linear. Then one easily checks that $[\cdot, \cdot]_G$ is a Lie bracket on $|\mathbb{C}\pi|$.

The original definition of the Turaev cobracket is similar, but uses self intersections of a curve in place of the intersections between two curves. Unfortunately, it is not well-defined with respect to the Reidemeister 1 relation for free homotopy curves, hence the need for the enhancement. We construct the (enhanced) co-bracket via a self-intersection map for *based* curves, as in [AKKN18b, Section 5.2]; this definition lends itself well to direct comparison with the three-dimensional operations of Section 5. For a based curve γ in $\mathbb{C}\pi$, the idea is to “snip off” portions of γ at self intersection points to get two curves, one of which is based and the other free. Figure 5 shows an example.

The sign here (with the minus sign in front) matches with AKKN genus 0, but is the opposite of AKKN higher genus and Goldman’s original definition. Our current multiplication and bracket matches the sign here, so if we change the sign then we should change the stacking order of our multiplication.

def:mu

Definition 3.3 (The self-intersection map). For $\gamma \in \mathbb{C}\pi$, let $\tilde{\gamma} \in \mathbb{C}\tilde{\pi}$ denote a path such that $\tilde{\gamma}\nu$ is homotopic to γ ; and such that $\tilde{\gamma}$ has only transverse double points, and $\text{rot}(\tilde{\gamma}) = 1/2$ (hence, $\text{rot}(\tilde{\gamma}\nu) = 0$). Let $\tilde{\gamma} \cap \tilde{\gamma}$ denote the set of double points. The self intersection map μ is defined as follows:

$$\mu : \mathbb{C}\pi \rightarrow |\mathbb{C}\pi| \otimes \mathbb{C}\pi$$

$$\mu(\gamma) = - \sum_{p \in \tilde{\gamma} \cap \tilde{\gamma}} \epsilon_p |\tilde{\gamma}_{t_1^p t_2^p}| \otimes \tilde{\gamma}_{0 t_1^p} \tilde{\gamma}_{t_2^p 1},$$

where t_1^p and t_2^p are the first and second time parameter in $[0, 1]$ where $\tilde{\gamma}$ goes through p ; where $\tilde{\gamma}_{rs}$ denotes the path traced by $\tilde{\gamma}$ from $t = r$ to $t = s$; the sign $\epsilon_p = \epsilon(\dot{\tilde{\gamma}}(t_1^p), \dot{\tilde{\gamma}}(t_2^p)) \in \{\pm 1\}$ is the local self-intersection number; and the formula extends to $\mathbb{C}\pi$ linearly.

The Turaev cobracket is obtained from μ by closing off the path component and making the tensor product alternating: this descends to a map on $|\mathbb{C}\pi|$, as follows.

def:cobrac

Definition 3.4. [The Turaev co-bracket] The Turaev cobracket δ is the unique linear map which makes the following diagram commute, where $\text{Alt}(x \otimes y) = x \otimes y - y \otimes x = x \wedge y$, and $\bar{\delta}$ denotes the composition of μ with closure, alternation

and a framing correction, as shown:

$$\begin{array}{ccccc}
 \gamma \in \mathbb{C}\pi & \xrightarrow{\mu} & |\mathbb{C}\pi| \otimes \mathbb{C}\pi & \xrightarrow{1 \otimes |\cdot|} & |\mathbb{C}\pi| \otimes |\mathbb{C}\pi| \\
 \downarrow |\cdot| & \searrow \tilde{\delta} & & & \downarrow \text{Alt} \\
 & & & & |\mathbb{C}\pi| \wedge |\mathbb{C}\pi| \\
 & & & & \downarrow +|\gamma| \wedge 1 \\
 |\mathbb{C}\pi| & \xrightarrow{\delta} & & & |\mathbb{C}\pi| \wedge |\mathbb{C}\pi|
 \end{array}$$

sec:gr_bialgebra

3.3. Associated graded Goldman-Turaev Lie bialgebra. There I-adic filtration on $\mathbb{C}\pi$ is the filtration by powers of the augmentation ideal $\mathcal{I} = \langle \{\alpha - 1\}_{\alpha \in \pi} \rangle$:

$$\mathbb{C}\pi = \mathcal{I}^0 \supseteq \mathcal{I} \supseteq \mathcal{I}^2 \supseteq \dots$$

By the 1930's work of Magnus [Mag35], the associated graded algebra of $\mathbb{C}\pi$ with respect to this filtration is the degree completed free algebra $\text{FA} = \text{FA}\langle x_1, \dots, x_p \rangle$:

Proposition 3.5. *Given the set of standard generators $\{\gamma_i\}_{i=1}^p$ for π , there is an isomorphism of algebras $\text{gr } \mathbb{C}\pi \rightarrow \text{FA}$ and the exponential expansion $\varphi(\gamma_i^{\pm 1}) = e^{\pm x_i}$ is a homomorphic expansion.*

The I-adic filtration of $\mathbb{C}\pi$ descends to a filtration on $|\mathbb{C}\pi|$:

$$|\mathbb{C}\pi| = |\mathcal{I}^0| \supseteq |\mathcal{I}| \supseteq |\mathcal{I}^2| \supseteq \dots$$

The completed associated graded vector space for $|\mathbb{C}\pi|$ with respect to this filtration is, by definition

$$\text{gr } |\mathbb{C}\pi| = \prod_{n=0}^{\infty} |\mathcal{I}^n| / |\mathcal{I}^{n+1}|.$$

There is an isomorphism $\text{gr } |\mathbb{C}\pi| \cong |\text{FA}|$, where $|\text{FA}|$ denotes the linear quotient $|\text{FA}| = \text{FA} / [\text{FA}, \text{FA}]$, and the exponential expansion descends to a homomorphic expansion for $|\mathbb{C}\pi|$. The vector space $|\text{FA}|$ is spanned by cyclic words in letters x_1, \dots, x_p , that is, words modulo cyclic permutations of the letters.

Therefore, $|\text{FA}|$ carries the structure of a Lie bialgebra under $\text{gr}[\cdot, \cdot]_G$ and $\text{gr } \delta$ [AKKN18a, Section 3]. Note that the Goldman bracket and the Turaev co-bracket are not strictly filtered maps, as they both shift filtered degree down by one⁵. For example, if $x \in |\mathcal{I}^r|$ and $y \in |\mathcal{I}^s|$, then $[x, y]_G \in |\mathcal{I}^{r+s-1}|$. Correspondingly, the associated graded operations are maps of degree -1 .

Figure 6 shows a schematic calculation of the graded Goldman bracket, with cyclic words represented diagrammatically as letters along a circle. The graded Goldman bracket sums over matching pairs of letters in z and w , joins the circles at the matching letter, and takes the difference of the two ways of including

⁵In [AKKN18a, Sections 3.3, 3.4] the down-shifts are by up to two filtered degrees, as the generating curves around genera and those around boundary components carry different weights. In our genus zero setting this translates to a degree shift of -1 .

$$\left[\text{circle with } x, \text{ circle with } x \right]_{\text{gr } G} = \sum_{\text{matching pairs}} \text{diagram 1} - \text{diagram 2}$$

FIGURE 6. A schematic diagrammatic example of the graded Goldman bracket.

fig:grbracket

$$\sum_{\text{pairing cuts}} \text{arc with } x \otimes \text{arc} - \text{arc} \otimes \text{arc with } x$$

FIGURE 7. A schematic diagrammatic example of the graded Self-intersection map, $\text{gr } \mu$.

fig:grmu

only one copy of the letter in the new cyclic word. Stated algebraically, this is summarised as follows:

Proposition 3.6. [AKKN18a, Section 3.3] Let $z = |z_1 \cdots z_l|$ and $w = |w_1 \cdots w_m|$ be two cyclic words in $|\text{FA}|$. The graded Goldman bracket

$$\text{gr}([-, -]_G) = [-, -]_{\text{gr } G} : |\text{FA}| \otimes |\text{FA}| \rightarrow |\text{FA}|$$

is given by:

$$[z, w]_{\text{gr } G} = \sum_{j,k} \delta_{z_j, w_k} (|w_1 \cdots w_{k-1} z_{j+1} \cdots z_l z_1 \cdots z_j w_{k+1} \cdots w_m| - |w_1 \cdots w_{k-1} z_j \cdots z_l z_1 \cdots z_{j-1} w_{k+1} \cdots w_m|),$$

where δ_{z_j, w_k} is the Kronecker delta.

Figure 7 shows a schematic diagrammatic calculation of the graded self-intersection map μ_{gr} , as a sum over *pairing cuts*. A pairing cut identifies two matching letters in a word, and splits the word along a chord connecting these matching letters. The graded self-intersection map outputs the tensor product of the resulting cyclic word and the remainder of the associative word. (The framing term $|\gamma| \wedge 1$ in the definition of δ does not contribute to the associated graded cobracket, since it is in filtered degree 0.) In summary:

prop:gr_mu

Proposition 3.7. [AKKN18a, Section 3.4] Let $w = w_1 \cdots w_m \in \text{As}_p$. The graded self-intersection map

$$\text{gr}(\mu) = \mu_{\text{gr}} : |\text{FA}| \rightarrow |\text{FA}| \otimes |\text{FA}|$$

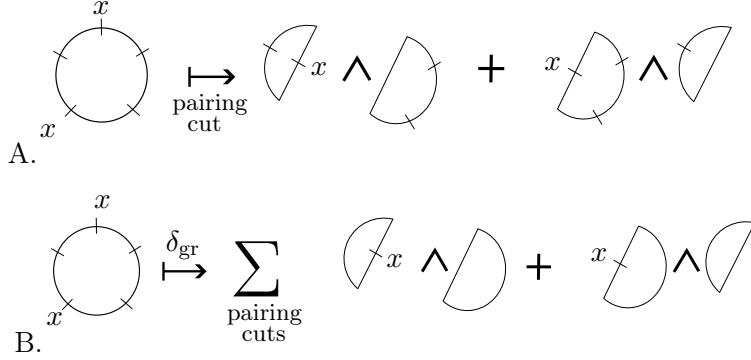


FIGURE 8. (A.) An example pairing cut of a cyclic word. (B.) An example of the graded Turaev cobracket as a sum over pairing cuts of a cyclic word.

fig:paircut

is given by:

$$\mu_{\text{gr}}(w) = \sum_{j < k} \delta_{w_j, w_k} (|w_j \dots w_{k-1}| \otimes w_1 \dots w_{j-1} w_{k+1} \dots w_m - |w_{j+1} \dots w_{k-1}| \otimes w_1 \dots w_j w_{k+1} \dots w_m),$$

where δ_{w_j, w_k} denotes the Kronecker delta.

Figure 8(A.) shows a schematic diagrammatic definition of the graded Turaev co-bracket, again as a sum over *pairing cuts*. A pairing cut in a cyclic word identifies a pair of coinciding letters, and cuts the cycle into two cycles along the chord connecting the matching letters. To obtain the cobracket, one takes a sum of wedge products of the resulting split cyclic words, adding one copy of the coinciding letter to either side, as shown in Figure 8(B.) and expressed in formulas below:

prop:gr_del

Proposition 3.8. [AKKN18a, Section 3.4] Let $w = w_1 \dots w_m \in |As_p|$. The graded Turaev cobracket

$$\text{gr}(\delta) = \delta_{\text{gr}} \otimes |FA| \rightarrow |FA| \wedge |FA|$$

is given by

$$\delta_{\text{gr}}(w) = \sum_{j < k} \delta_{w_j, w_k} (|w_j \dots w_{k-1}| \wedge |w_{k+1} \dots w_m w_1 \dots w_{j-1}| + |w_k \dots w_m w_1 \dots w_{j-1}| \wedge |w_{j+1} \dots w_{k-1}|),$$

where δ_{w_j, w_k} denotes the Kronecker delta⁶.

⁶Apologies for the notation clash.

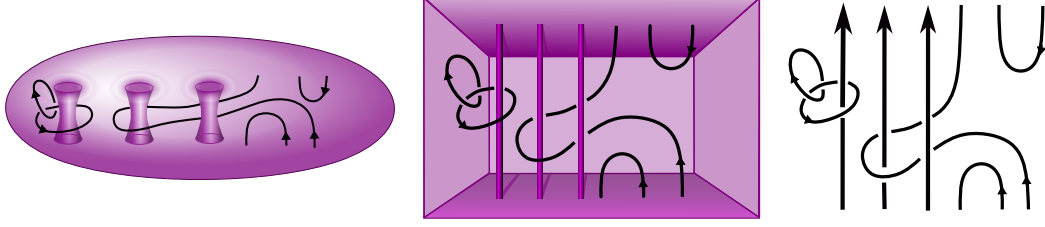


FIGURE 9. An example of a tangle in M_3 , drawn first in a handlebody, then in a cube with poles, and lastly as a tangle diagram projected to the back wall of the cube.

fig:polestudio

4. EXPANSIONS FOR TANGLES IN HANDLEBODIES

4.1. Framed oriented tangles. This section introduces the space \mathcal{CT} of framed, oriented tangles in a genus p handlebody, with formal linear combinations. Our main result – proven in Section 5 – is that homomorphic expansions on \mathcal{CT} induce homomorphic expansions on the Goldman-Turaev Lie biagebra.

Let M_p denote the manifold $D_p \times I$ where D_p is a disc in the complex plane with p points removed. While M_p is not a compact manifold, knot theory in M_p is equivalent to knot theory in a genus p handlebody. For the purpose of the Kontsevich integral, we identify D_p with a unit square $[0, 1] + [0, i]$ in the complex plane with p points removed, so M_p can be drawn as a cube with p vertical lines removed; we call these lines *poles*, as shown in the middle in Figure 9. We refer to $D_p \times \{0\}$ as the “floor” or “bottom”, and $D_p \times \{1\}$ as the “ceiling” or “top”. The “back wall” is the face $[i, i + 1] \times [0, 1]$. We refer to the $i \in \mathbb{C}$ direction as North.

def:tangle

Definition 4.1. An oriented tangle T in M_p is an embedding of an oriented compact 1-manifold

$$(S, \partial S) \hookrightarrow (M_p, D_p \times \{0\} \cup D_p \times \{1\}).$$

The interior of S lies in the interior of M_p , and the boundary points of S are mapped to the top or bottom. Oriented tangles in M_p are considered up to ambient isotopy fixing the boundary. We denote the set of isotopy classes by \mathcal{T} . An example is shown in Figure 9.

def:framed_tangles

Definition 4.2. A *framing* for an oriented tangle T in M_p is a continuous choice of unit normal vector at each point of T , which is fixed pointing North at the boundary points. *Framed oriented tangles* in M_p are also considered up to ambient isotopy fixing the boundary. We denote the set of isotopy classes of framed oriented tangles by $\tilde{\mathcal{T}}$.

Henceforth, any tangle is assumed to be framed and oriented unless otherwise stated. The skeleton of a tangle is the underlying combinatorial information with the topology forgotten:

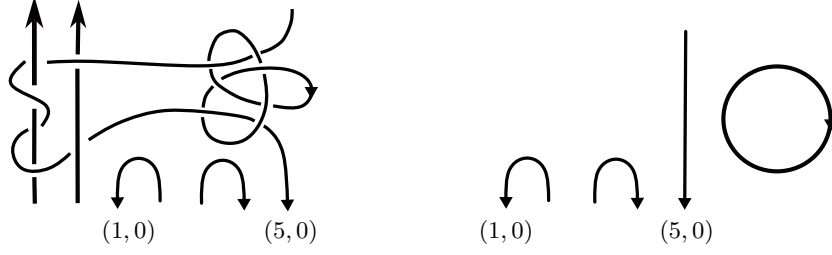


FIGURE 10. On the left is a tangle in M_2 , and on the right is schematic diagram of the skeleton of the tangle. The skeleton of the tangle is the combinatorial data given by the following set of order pairs and the integer 1: $\{[(2, 0), 0], [(1, 0), 0)], [((3, 0), 0), (4, 0), 0)], [((5, 0), 1), (5, 0), 0)], 1\}$

fig:skeleton

def:skeleton

Definition 4.3. The *skeleton* $\sigma(T)$ of a tangle $T = (S \hookrightarrow M_p)$ – see Figure 10 – is the set of tangle endpoints $P_{bot} \subseteq D_p \times \{0\}$ and $P_{top} \subseteq D_p \times \{1\}$, along with

- (1) A partition of $P_{bot} \cup P_{top}$ into ordered pairs given by the oriented intervals of S .
- (2) A non-negative integer k : the number of circles in S .

The skeleton of a framed tangle is the same as the skeleton of the underlying unframed tangle. The set of framed tangles in M_p with skeleton S is denoted $\tilde{\mathcal{T}}(S)$. For example, $\tilde{\mathcal{T}}(\bigcirc)$ is the set of framed knots in M_p .

The linear extension of $\tilde{\mathcal{T}}(S)$, denoted $\mathbb{C}\tilde{\mathcal{T}}(S)$, is the vector space of \mathbb{C} -linear combinations of tangles in $\tilde{\mathcal{T}}(S)$. We denote by $\mathbb{C}\tilde{\mathcal{T}}$ the disjoint union $\sqcup_S \mathbb{C}\tilde{\mathcal{T}}(S)$ over all skeleta S . Tangles with different skeleta cannot be linearly combined.

One may represent tangles in M_p using tangle diagrams in (at least) two different ways: by projecting to the back wall of M_p or to the floor.

Projecting to the back wall, an ℓ -component tangle in M_p can be diagrammatically represented as a tangle diagram with p straight vertical *poles*, and ℓ *tangle strands* of circle and interval components. The strands pass over (in front of) and under (behind) the poles and other strands, as shown on the right in Figure 9. The poles are oriented upwards. By Reidemeister's theorem, $\tilde{\mathcal{T}}$ is in bijection with such diagrams modulo the Reidemeister moves R2 and R3, and the framed version of R1.

By projecting instead to the floor $D_p \times \{0\}$, a tangle in M_p is represented by a tangle diagram in D_p . The R2 and R3 moves continue to apply. The endpoints of the tangle are fixed: bottom endpoints are denoted by dots, top endpoints are denoted by stars. Strands of the tangle diagram can pass over bottom endpoints, or under top endpoints, as shown in Figure 11. However, the strands cannot pass across the punctures in D_p .

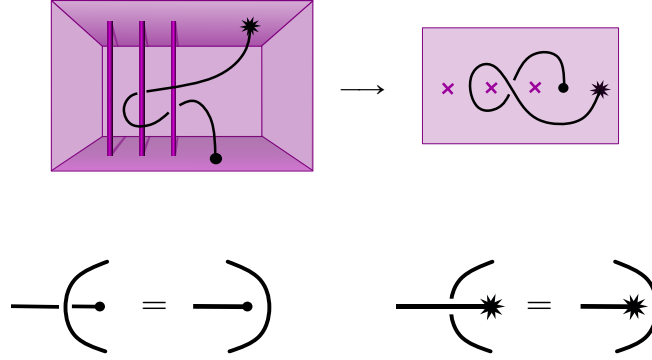


FIGURE 11. An example of a tangle in M_3 projected to the bottom floor of the cube. Strands of a tangle diagram can pass over bottom endpoints (dot) or under top endpoints (star).

fig:BottomDiagram

sec:opsonT

4.2. Operations on $\tilde{\mathcal{T}}$. There are several useful operations defined on $\tilde{\mathcal{T}}$. These operations extend linearly to $\mathbb{C}\tilde{\mathcal{T}}$, and are used in Section 5 to relate quotients of $\mathbb{C}\tilde{\mathcal{T}}$ to the Goldman-Turaev Lie bialgebra.

- *Stacking product:* Given tangles $T_1, T_2 \in M_p$, if the top endpoints of $\sigma(T_1)$ coincide with the bottom endpoints of $\sigma(T_2)$ in D_p , and the orientations on the strands of T_1 and T_2 agree, then the product $T_1 T_2$ is the tangle obtained by stacking T_2 on top of T_1 .
- *Strand addition:* The *strand addition* operation adds a non-interacting additional strand to a tangle T at a point $q \in D_p$ to get a new tangle $T \sqcup_q \uparrow$. More precisely, pick a contractible $U \subseteq D_p$ such that T is contained entirely in $U \times [0, 1]$ and a point $q \in D_p$ outside of U . The tangle $T \sqcup_q \uparrow$ is T together with an upward-oriented vertical strand $q \times I$ at q .
- *Strand orientation switch:* This operation reverses the orientation of a given strand of the tangle.
- *Flip:* Given a tangle T in M_p , the flip of a tangle T in M_p , denoted T^\sharp , is the mirror image of T with respect to the ceiling, as shown in Figure 12. When T is flipped, each top boundary point $(q, 1)$ becomes a bottom boundary point $(q, 0)$, and vice versa. The orientations and framing of the strands of T are reflected along with the strands. However, the orientations of the poles remain ascending. Equivalently, the flip operation can be defined as reversing the parametrisation of I in $M_p \cong D_p \times I$. This, in effect, flips the orientation of the poles but changes nothing else.

In Section 5.1, we show that the stacking commutator of tangles, given by $[T_1, T_2] = T_1 T_2 - T_2 T_1$, induces to the Goldman bracket in the sense of Section 2.

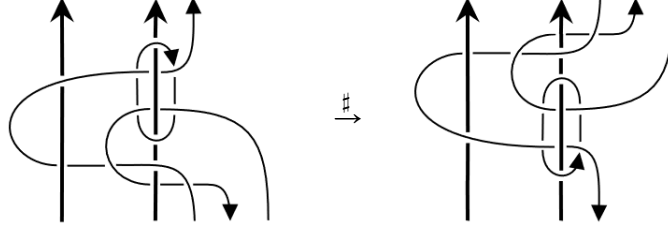
FIGURE 12. A tangle in M_2 and its flip

fig:flip

In Section 5.2 a similar but more subtle argument relates the flip operation to the Turaev cobracket.

sec:t-filtration

4.3. The t -filtration on $\tilde{\mathcal{T}}$ and the associated graded $\tilde{\mathcal{A}}$. In setting up a theory of Vassiliev invariants for $\tilde{\mathcal{T}}$, there are different filtrations to consider. In line with classical notation of Vassiliev invariants, we denote by a double point the difference between an over-crossing and an under-crossing:

$$\bowtie = \nearrow \searrow - \searrow \nearrow.$$

Double points, however, come in two varieties: *pole-strand*, if the crossing occurs between a pole and a tangle strand, and *strand-strand*, if the crossing occurs between two tangle strands. As the poles are fixed, they never cross each other, hence, there are no pole-pole double points.

The main filtration we consider on $\mathbb{C}\tilde{\mathcal{T}}$ is the filtration by the total number of double points of either type, as well as strand framing changes (as in Section 3.1). We call this the *total filtration*, or t -filtration for short, and write it as

$$\mathbb{C}\tilde{\mathcal{T}} = \tilde{\mathcal{T}}_0 \supseteq \tilde{\mathcal{T}}_1 \supseteq \tilde{\mathcal{T}}_2 \supseteq \tilde{\mathcal{T}}_3 \supseteq \cdots$$

where $\tilde{\mathcal{T}}_t$ is the set of linear combinations of framed tangle diagrams with at least t total double points and strand framing changes. In spirit, this filtration comes from the diagrammatic view of projecting to the back wall of the cube.

The associated graded space of $\mathbb{C}\tilde{\mathcal{T}}$ with respect to the total filtration is

$$\tilde{\mathcal{A}} := \text{gr } \mathbb{C}\tilde{\mathcal{T}} = \prod_{t \geq 0} \tilde{\mathcal{T}}_t / \tilde{\mathcal{T}}_{t+1}.$$

The degree t component of $\tilde{\mathcal{A}}$ is $\tilde{\mathcal{A}}_t := \tilde{\mathcal{T}}_t / \tilde{\mathcal{T}}_{t+1}$.

As in classical Vassiliev theory (cf. section 3.1), the associated graded space $\tilde{\mathcal{A}}$ has a combinatorial description in terms of *chord diagrams*.

Definition 4.4. A *chord diagram* on a tangle skeleton is an even number of marked points on the poles and skeleton strands, up to orientation preserving diffeomorphism, along with a perfect matching on the marked points – that is, a partition of marked points into unordered pairs. In diagrams, the pairs are connected by a *chord*, indicated by a dashed line, as in Figure 13.

Dror thinks we should
remove the last sentence

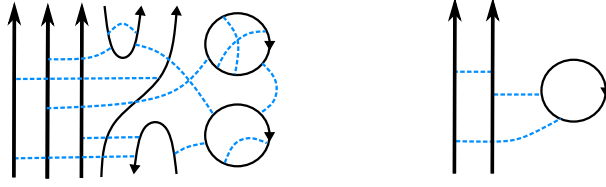


FIGURE 13. Two chord diagrams: an admissible one (left), and a non-admissible one (right) that does contain a pole-pole chord.

ssibleNonAdmissible

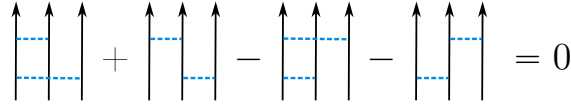


FIGURE 14. The 4T relation, which is admissible if at most one of the three skeleton components is a pole.

fig:Admissible 4T

def:admissible

Definition 4.5. A chord diagram is *admissible* if all chords connect strands to strands, or strands to poles, but there are no pole-pole chords. See Figure 13 for examples.

def:cdspace

Definition 4.6. The space $\mathcal{D}(S)$ of *admissible chord diagrams on a skeleton* S is the space of \mathbb{C} -linear combinations of admissible chord diagrams on the skeleton S , modulo *admissible 4T* relations, shown in Figure 14. Admissible 4T relations are 4T relations where all four terms are admissible⁷. That is,

$$\mathcal{D}(S) = \frac{\langle \text{admissible chord diagrams on } S \rangle}{\{\text{admissible 4T relations}\}}$$

The space $\mathcal{D}(S)$ is a graded vector space, where the degree is given by the number of chords. Denote the degree t component of $\mathcal{D}(S)$ by $\mathcal{D}_t(S)$. Let \mathcal{D} denote the disjoint union $\sqcup_S \mathcal{D}(S)$, and denote the degree t component of \mathcal{D} by $\mathcal{D}_t \doteq \sqcup_S \mathcal{D}_t(S)$.

The well-known map $\psi : \mathcal{D} \rightarrow \tilde{\mathcal{A}}$ from classical Vassiliev theory is defined as follows. In degree t , $\psi_t : \mathcal{D}_t \rightarrow \tilde{\mathcal{T}}_t / \tilde{\mathcal{T}}_{t+1}$, “contracts” the t chords to double points, as shown in Figure 15. This may create other crossings, but modulo $\tilde{\mathcal{T}}_{t+1}$ the over/under information at these crossings does not matter.

lem:psi

Lemma 4.7. *The map ψ is well-defined and surjective.*

Proof. To show ψ is well-defined, it suffices to show that admissible 4T relations in \mathcal{D}_t are in the kernel of ψ . This is the standard “lasso trick” recalled in Figure 16. For surjectivity, recall from Section 3.1.2 that a framing change in $\tilde{\mathcal{A}}$ is half of

citation needed

⁷Equivalently, a 4T relation is admissible if at most one of the three skeleton components involved is a pole.

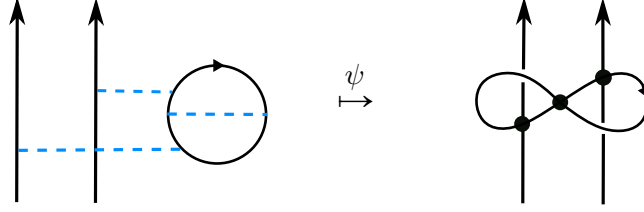


FIGURE 15. Example of ψ with the right hand side viewed as an element of $\tilde{\mathcal{T}}_3/\tilde{\mathcal{T}}_4$. Different choices of over or under crossings with the poles only differ by elements of $\tilde{\mathcal{T}}_4$.

fig:psi

$$\begin{aligned} \psi \left(- \begin{array}{c} \uparrow \uparrow \uparrow \\ \text{---} \text{---} \text{---} \\ \uparrow \uparrow \uparrow \end{array} + \begin{array}{c} \uparrow \uparrow \uparrow \\ \text{---} \text{---} \text{---} \\ \uparrow \uparrow \uparrow \end{array} + \begin{array}{c} \uparrow \uparrow \uparrow \\ \text{---} \text{---} \text{---} \\ \uparrow \uparrow \uparrow \end{array} - \begin{array}{c} \uparrow \uparrow \uparrow \\ \text{---} \text{---} \text{---} \\ \uparrow \uparrow \uparrow \end{array} \right) &= - \begin{array}{c} \uparrow \uparrow \uparrow \\ \text{---} \text{---} \text{---} \\ \uparrow \uparrow \uparrow \end{array} + \begin{array}{c} \uparrow \uparrow \uparrow \\ \text{---} \text{---} \text{---} \\ \uparrow \uparrow \uparrow \end{array} + \begin{array}{c} \uparrow \uparrow \uparrow \\ \text{---} \text{---} \text{---} \\ \uparrow \uparrow \uparrow \end{array} - \begin{array}{c} \uparrow \uparrow \uparrow \\ \text{---} \text{---} \text{---} \\ \uparrow \uparrow \uparrow \end{array} \\ &= \begin{array}{c} \uparrow \uparrow \uparrow \\ \text{---} \text{---} \text{---} \\ \uparrow \uparrow \uparrow \end{array} - \begin{array}{c} \uparrow \uparrow \uparrow \\ \text{---} \text{---} \text{---} \\ \uparrow \uparrow \uparrow \end{array} = 0 \end{aligned}$$

FIGURE 16. Showing that $\psi : \mathcal{D} \rightarrow \tilde{\mathcal{A}}$ is well defined. The figure is understood locally: in degree t the chord diagrams have $t - 2$ other chords elsewhere, and correspondingly the tangles have $t - 2$ other double points elsewhere.

chord. So, both framing changes and double points are in the image of ψ , and thus ψ is surjective. \square

According to Lemma 3.1, in order to show that ψ is an isomorphism, one needs to find an expansion valued in \mathcal{D} .

thm:Zwelldefined

Lemma 4.8. *The framed Kontsevich integral $Z : \mathbb{C}\tilde{\mathcal{T}} \rightarrow \mathcal{D}$ satisfies the conditions of Lemma 3.1: it is filtered, and $\psi \circ \text{gr } Z = \text{id}_{\tilde{\mathcal{A}}}$.*

Proof. This is a variant of a standard fact [Kon93]; one detailed explanation is in [BN95, Section 4.3]. A small point to verify is that the image of Z on an element of $\mathbb{C}\tilde{\mathcal{T}}$ is an admissible chord diagram. This is immediate from the definition of the Kontsevich integral: the poles are parallel, hence the coefficient of a chord diagram with a pole-pole chord is computed by integrating zero. The main part, that $\psi \circ \text{gr } Z = \text{id}_{\tilde{\mathcal{A}}}$, is done as in [BN95, Section 4.4.2, Thm 1 part (3)]. \square

The next corollary is then immediate from Lemma 3.1:

cor:grcd

Corollary 4.9. *The map $\psi : \mathcal{D} \rightarrow \tilde{\mathcal{A}}$ is an isomorphism, and Z is an expansion for $\tilde{\mathcal{T}}$.*

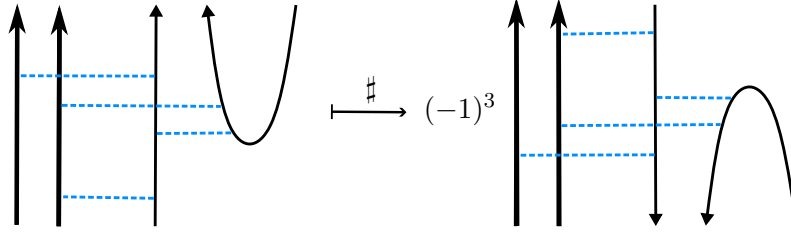


FIGURE 17. An example chord diagram and its flip.

chorddiagoperations

After identifying $\tilde{\mathcal{A}}$ with \mathcal{D} , the degree t component of $\tilde{\mathcal{A}}$, $\tilde{\mathcal{A}}_t = \tilde{\mathcal{T}}_t / \tilde{\mathcal{T}}_{t+1}$, consists of all admissible chord diagrams in $\tilde{\mathcal{A}}$ with exactly t chords.

For a skeleton S , we denote by $\tilde{\mathcal{A}}(S)$ the space of admissible chord diagrams on the skeleton S , so $\tilde{\mathcal{A}}(S)$ is the associated graded vector space of $\mathbb{C}\tilde{\mathcal{T}}(S)$. For example, $\tilde{\mathcal{A}}(\bigcirc)$ is the associated graded vector space of the space of knots in M_p .

4.4. Operations on $\tilde{\mathcal{A}}$. The tangle operations *stacking*, *strand addition*, *strand orientation switch*, and *flip* on $\tilde{\mathcal{T}}$ induce associated graded operations by the same names on $\tilde{\mathcal{A}}$. In view of Corollary 4.9, we give descriptions of these operations using chord diagrams.

The operation *stacking* is given by concatenating the skeleta of two chord diagrams (as long as they have the same number of poles, and the top endpoints of one match the bottom endpoints of the other, including orientations).

The associated graded *strand addition* operation adds a vertical skeleton strand to a chord diagram. The new strand has no chord endings.

The associated graded *strand orientation switch* for strand e switches the orientation of the strand e , and multiplies each chord diagram with (-1) to the power of the number of chord endings on e . The sign arises from the fact that reversing the orientation of e changes the signs of double points between e and any other distinct strand or pole.

The associated graded operation *flip*, denoted by \sharp , reflects a chord diagram with respect to a “mirror on the ceiling”; then reverses the orientations of the poles so that they are oriented upwards, as in see Figure 17; and multiplies by a factor of $(-1)^m$, where m is the total number of chord endings on the poles. The factor of $(-1)^m$ arises from the pole orientation reversals, as this changes the signs of any pole-strand double points. 17.

The following proposition is straightforward from the definition of Z .

prop:Zhomom

Proposition 4.10. *The Kontsevich integral Z intertwines stacking, strand additions, orientation reversals and flips with their associated graded operations.* \square

4.5. The s -filtration on $\tilde{\mathcal{T}}$ and $\tilde{\mathcal{A}}$. Recall from Section 4.3 that the total filtration on $\mathbb{C}\tilde{\mathcal{T}}$ is given by strand framing changes and double points between strands

sec:s-sfiltration

with poles and strands with strands. In this section we introduce a second filtration on $\mathbb{C}\tilde{\mathcal{T}}$, given by strand framing changes, and *only strand-strand* double points. We call this the *strand filtration*, or simply *s-filtration*.

We use subscripts for the *s*-filtration:

$$\mathbb{C}\tilde{\mathcal{T}} = \tilde{\mathcal{T}}^0 \supseteq \tilde{\mathcal{T}}^1 \supseteq \tilde{\mathcal{T}}^2 \supseteq \tilde{\mathcal{T}}^3 \supseteq \dots,$$

where $\tilde{\mathcal{T}}^s \subseteq \mathbb{C}\tilde{\mathcal{T}}$ is spanned by tangles with at least s strand framing changes or strand double points.

Remark 4.11. The associated graded structure of $\mathbb{C}\tilde{\mathcal{T}}$ with respect to the *s*-filtration was studied by Habiro and Massuyeau in [HM21], as part of their work on *bottom tangles*⁸. Yet we do not apply the associated graded functor to the *s*-filtration, but rather, quotient only by $\tilde{\mathcal{T}}^1$ and $\tilde{\mathcal{T}}^2$ to identify the Goldman-Turaev spaces and operations in Section 5.

In turn, the *s*-filtration induces a filtration on $\tilde{\mathcal{A}}$, as follows. Let $\tilde{\mathcal{T}}_t^s$ denote $\tilde{\mathcal{T}}_t \cap \tilde{\mathcal{T}}^s$: that is, the linear span of tangles in $\mathbb{C}\tilde{\mathcal{T}}$, which that have at least t double points or framing changes, at least s of which are strand-strand double points or framing changes.

Definition 4.12. Denote by $\tilde{\mathcal{A}}^{\geq s}$ the *s*-filtered component of $\tilde{\mathcal{A}}$:

$$\tilde{\mathcal{A}}^{\geq s} := \prod \tilde{\mathcal{T}}_t^s / \tilde{\mathcal{T}}_{t+1}^s.$$

Explicitly, $\tilde{\mathcal{A}}^{\geq s}$ is spanned by chord diagrams with at least s strand-strand chords.

For strand-strand chords we will use the shorthand word *s*-chords. Note that the number of *s*-chords is only a filtration, not itself grading on $\tilde{\mathcal{A}}$, as the 4T relation is not homogeneous with respect to the number of *s*-chords.

Proposition 4.13. *The Kontsevich integral Z is a filtered map with respect to the *s*-filtration.*

Proof. This is a close analogue of Theorem 4.8. As strand-strand double points correspond to strand-strand chords via the identification ψ of the associated graded space with chord diagrams, the proof translates verbatim from [BN95, Section 4.3]. \square

4.6. The Conway quotient. In this section we introduce the last necessary ingredient for identifying the Goldman-Turaev operations: the Conway quotient of $\mathbb{C}\tilde{\mathcal{T}}$. This is essentially the Conway skein module of tangles in M_p , but without fixing the value of the unknot. We show that the Kontsevich integral descends to the Conway quotient.

⁸Projecting to the bottom of the cube rather than the back wall makes the strand filtration the natural Vassiliev filtration to consider.

this might be a good place to add a remark about how emergent knots arise in this context.

ionQuotientNotation

prop:ZrespectsS

sec:Conway

def:conway

Definition 4.14. The Conway quotient of $\mathbb{C}\tilde{\mathcal{T}}$, denoted $\mathbb{C}\tilde{\mathcal{T}}_\nabla$, is given by

$$\mathbb{C}\tilde{\mathcal{T}}_\nabla := \mathbb{C}\tilde{\mathcal{T}}[a] / \left(\text{strand-strand crossing} - \text{strand-strand crossing} = (e^{\frac{a}{2}} - e^{-\frac{a}{2}}) \right),$$

where a is a formal variable of t and s degree 1, and the skein relation is restricted to strand-strand crossings. We use the shorthand $b := e^{\frac{a}{2}} - e^{-\frac{a}{2}}$.

The t and s filtrations on $\mathbb{C}\tilde{\mathcal{T}}$ induce filtrations on $\mathbb{C}\tilde{\mathcal{T}}_\nabla$. Let $\tilde{\mathcal{T}}_\nabla^s$ denote the s -filtered component in the s -filtration of $\mathbb{C}\tilde{\mathcal{T}}_\nabla$. Let $\tilde{\mathcal{T}}_{\nabla,t}$ denote the t -filtered component in the total filtration of $\mathbb{C}\tilde{\mathcal{T}}_\nabla$, and $\tilde{\mathcal{A}}_\nabla := \text{gr}_t \mathbb{C}\tilde{\mathcal{T}}_\nabla = \coprod \tilde{\mathcal{T}}_{\nabla,t} / \tilde{\mathcal{T}}_{\nabla,t+1}$ denote the associated graded algebra of $\mathbb{C}\tilde{\mathcal{T}}_\nabla$ with respect to the total filtration. Let $\tilde{\mathcal{A}}_{\nabla,t}$ denote the degree t component of $\tilde{\mathcal{A}}_\nabla$, $\tilde{\mathcal{A}}_\nabla^s$ be the s -th filtered component, and $\tilde{\mathcal{A}}_{\nabla,t}^s := \tilde{\mathcal{A}}_{\nabla,t} \cap \tilde{\mathcal{A}}_\nabla^s$. We now show that $\tilde{\mathcal{A}}_\nabla$ has a chord diagrammatic description similar to Corollary 4.9. Recall that \mathcal{D} is the space of chord diagrams on tangle skeleta, modulo admissible 4T relations.

def:D_con

Definition 4.15. The Conway quotient of \mathcal{D} is given by

$$\mathcal{D}_\nabla := \mathcal{D}[a] / \left(\text{relation 1} = a \text{relation 2}, \text{relation 3} = a \text{relation 4} \right)$$

where the new relations are restricted to chords on strand skeleton components (not poles).

Note that the two new relations in \mathcal{D}_∇ are equivalent, shown in both combinations of orientations for convenience. Furthermore, the relations are homogeneous (respect the t -grading) on \mathcal{D} , and therefore \mathcal{D}_∇ is also graded by the sum of the total number of chords and the exponent of a . The next theorem shows that $\tilde{\mathcal{A}}_\nabla \cong \mathcal{D}_\nabla$: this essentially follows from the results of [LM95]. For completeness we present a direct proof.

thm:Z_conway

Theorem 4.16. The isomorphism ψ descends to an isomorphism $\psi_\nabla : \tilde{\mathcal{A}}_\nabla \cong \mathcal{D}_\nabla$, and the Kontsevich integral descends to an expansion $Z_\nabla : \mathbb{C}\tilde{\mathcal{T}}_\nabla \rightarrow \mathcal{D}_\nabla$.

Proof. First we show that ψ descends to a surjective graded map $\psi : \mathcal{D}_\nabla \rightarrow \tilde{\mathcal{A}}_\nabla$. To show that ψ is well-defined, we need to show that the Conway relations in \mathcal{D}_∇ is in the kernel. We verify one of the two equivalent relations:

$$\psi \left(\text{relation 1} - a \text{relation 2} \right) = \text{relation 1} - a \text{relation 2} = a \text{relation 3} - a \text{relation 4} = 0.$$

Next, we verify that the Kontsevich integral Z descends to a map $\mathbb{C}\tilde{\mathcal{T}}_\nabla \rightarrow \tilde{\mathcal{A}}_\nabla$ by verifying the relations in $\mathbb{C}\tilde{\mathcal{T}}_\nabla$. We do this first at the level of tangles with two bottom and two top endpoints (directly above). Recall that the Kontsevich integral is invariant under both total horizontal and total vertical rescaling, and hence well-defined for such two-two tangles without specifying the distance between the endpoints.

Recall that

$$Z(\text{strand-strand crossing}) = \left(e^{\frac{c}{2}} \right) \cdot \text{strand-strand crossing}, \quad \text{and} \quad Z(\text{strand-strand crossing}) = \left(e^{-\frac{c}{2}} \right) \cdot \text{strand-strand crossing},$$

where C denotes a chord, the exponential is interpreted formally as a power series with the stacking multiplication, as shown in the first equality below. Using the Conway relation, we compute:

$$C^k = \left\{ \begin{array}{c} \uparrow \\ \text{---} \\ \uparrow \end{array} \right\}_k \stackrel{\nabla}{=} a^k \left\{ \begin{array}{c} \uparrow \\ \text{---} \\ \uparrow \end{array} \right\}_k = a^k (\text{X})^k = \begin{cases} a^k \uparrow \uparrow, & \text{if } k \text{ is even} \\ a^k \text{X}, & \text{if } k \text{ is odd} \end{cases}$$

Now applying Z to the left hand side of the Conway relation, we obtain

$$\begin{aligned} Z(\text{X}) - Z(\text{X}) &= (e^{\frac{C}{2}} - e^{-\frac{C}{2}}) \text{X} \\ &= \sum_{k=0}^{\infty} \left(\frac{C^k}{2^k k!} - \frac{(-1)^k C^k}{2^k k!} \right) \text{X} = \sum_{k=0}^{\infty} \frac{C^{2k+1}}{2^{2k} (2k+1)!} \text{X} \\ &= \sum_{k=0}^{\infty} \frac{a^{2k+1} \text{X}}{2^{2k} (2k+1)!} \text{X} = \sum_{k=0}^{\infty} \frac{a^{2k+1}}{2^{2k} (2k+1)!} \uparrow \uparrow \\ &= (e^{\frac{a}{2}} - e^{-\frac{a}{2}}) \uparrow \uparrow \\ &= Z \left((e^{\frac{a}{2}} - e^{-\frac{a}{2}}) \uparrow \uparrow \right). \end{aligned}$$

To see that the local verification above is sufficient, one needs to recall more about the Kontsevich integral. Namely, Z is multiplicative with respect to the stacking composition of tangles (with fixed endpoints), and asymptotically commutes with “distant disjoint unions”, and these two facts imply the global equality (in fact, they lead to a combinatorial construction of Z for *parenthesised* tangles). For details see [CDM12, Chapter 8].

Therefore, by Lemma 3.1, Z is a (homomorphic) expansion for $\mathbb{C}\tilde{\mathcal{T}}_{\nabla}$ and $\psi : \mathcal{D}_{\nabla} \rightarrow \tilde{\mathcal{A}}_{\nabla}$ is an isomorphism. \square

Let $\boxed{\text{e}}$ denote the composition of the natural embedding with the Conway quotient map

$$\iota : \mathbb{C}\tilde{\mathcal{T}} \rightarrow \mathbb{C}\tilde{\mathcal{T}}[[a]] \rightarrow \mathbb{C}\tilde{\mathcal{T}}_{\nabla}.$$

The map ι is not injective, see for example Figure 18. However, it is surjective: all \mathbb{C} -linear combinations of tangles are in the image, and given a tangle T , $b^k T$ is equal in $\mathbb{C}\tilde{\mathcal{T}}_{\nabla}$ to a tangle with k double points, which is, in turn, a \mathbb{C} -linear combination of tangles.

`def:conway_skel`

Definition 4.17. For skeleton S , let $\boxed{\mathbb{C}\tilde{\mathcal{T}}_{\nabla}(S)}$ denote the image $\iota(\mathbb{C}\tilde{\mathcal{T}}(S))$.

Note that while the skeleton fibration of $\mathbb{C}\tilde{\mathcal{T}}$ is a partition into disjoint fibers $\mathbb{C}\tilde{\mathcal{T}}(S)$, this is no longer true in $\mathbb{C}\tilde{\mathcal{T}}_{\nabla}$ due to the non-injectivity of ι . For example, the middle term of the equality in Figure 18 lies in both $\mathbb{C}\tilde{\mathcal{T}}_{\nabla}(\bigcirc)$ and $\mathbb{C}\tilde{\mathcal{T}}_{\nabla}(\bigcirc\bigcirc\bigcirc)$.

Note that $\mathbb{C}\tilde{\mathcal{T}}_{\nabla}^{\vee} = \sum_s \mathbb{C}\tilde{\mathcal{T}}_{\nabla}(s)$ but not $\mathbb{C}\tilde{\mathcal{T}}_{\nabla}^{\vee} = \oplus \dots$

$$\begin{array}{c} \text{Diagram 1} \\ \cap \\ \mathbb{C}\tilde{\mathcal{T}}_{\nabla}(\bigcirc\bigcirc\bigcirc) \end{array} = b \cdot \left(\text{Diagram 2} \right) = \begin{array}{c} \text{Diagram 3} \\ \cap \\ \in \mathbb{C}\tilde{\mathcal{T}}_{\nabla}(\bigcirc) \end{array}$$

FIGURE 18. The map ι is not injective: The left hand side and the right hand side are both elements of $\mathbb{C}\tilde{\mathcal{T}}$, and equal in $\mathbb{C}\tilde{\mathcal{T}}_{\nabla}$.
Skeleta in the Conway quotient are not a partition.

fig:ConwaySkel

We will identify the Goldman-Turaev Lie bialgebra in low-degree quotients of the s -filtration of $\mathbb{C}\tilde{\mathcal{T}}_{\nabla}$. The next few propositions establish the necessary understanding of these quotients. Denote by $\tilde{\mathcal{T}}/\tilde{\mathcal{T}}^n$ the quotient $\tilde{\mathcal{T}}/\tilde{\mathcal{T}}^n$, and similarly for the Conway quotients, $\tilde{\mathcal{T}}_{\nabla}^n$ denotes $\mathbb{C}\tilde{\mathcal{T}}_{\nabla}/\tilde{\mathcal{T}}_{\nabla}^n$.

prop:nonabneeded

Proposition 4.18. *The map ι descends to a canonical isomorphism $\tilde{\mathcal{T}}_{\nabla}^1 \cong \tilde{\mathcal{T}}^1$.*

Proof. The Conway relation applies only in s -filtered degree one and higher, and hence has no effect on $\tilde{\mathcal{T}}^1$. \square

In light of this, we write only $\tilde{\mathcal{T}}^1$, rather than $\tilde{\mathcal{T}}_{\nabla}^1$. Now let $\tilde{\mathcal{T}}_{\nabla}^{1/2}$ denote $\tilde{\mathcal{T}}^1/\tilde{\mathcal{T}}_{\nabla}^2$, and $\tilde{\mathcal{T}}_{\nabla}^{1/2}$ denote $\tilde{\mathcal{T}}_{\nabla}^1/\tilde{\mathcal{T}}_{\nabla}^2$.

Finally, we establish a key technical result about low s -degree quotients of the Conway quotient:

Proposition 4.19. *The \mathbb{C} -linear map given by post-composing ι with multiplication⁹ by b ,*

$$\hat{b}: \tilde{\mathcal{T}}_{\nabla}^1 \rightarrow \tilde{\mathcal{T}}_{\nabla}^2$$

is injective, and its image is $\tilde{\mathcal{T}}_{\nabla}^{1/2}$.

Proof. We first prove that the image of \hat{b} is $\tilde{\mathcal{T}}_{\nabla}^{1/2}$. The quotient $\tilde{\mathcal{T}}^1$ is spanned by cosets of tangles T . It is immediate that the image of \hat{b} is contained in $\tilde{\mathcal{T}}_{\nabla}^{1/2}$, as $\hat{b}(T) = bT$ represents an element in $\tilde{\mathcal{T}}^1$.

Conversely, any element $y \in \tilde{\mathcal{T}}_{\nabla}^{1/2}$ is (non-uniquely) represented as a sum of the form $\sum_{i=1}^k T_i + b \sum_{j=1}^l T'_j$, where T_i are tangles with one double point each, and T'_j are arbitrary tangles. Then, by the Conway relation, each $T_i = b \cdot T_i^C$, where T_i^C denotes the tangle where the double point in T_i has been smoothed. Thus, $y = b \left(\sum_{i=1}^k T_i^C + \sum_{j=1}^l T'_j \right)$, and therefore y is in the image of \hat{b} , and \hat{b} is surjective onto $\tilde{\mathcal{T}}_{\nabla}^{1/2}$.

To prove the injectivity of \hat{b} , we construct a one-sided inverse: a “division by b ” map $\tilde{b}_{\text{on } \mathbb{C}\tilde{\mathcal{T}}_{\nabla}^2}$ as follows.

⁹In physics, multiplication by a variable b is denoted \hat{b} . Inspired by this notation, we will denote division by b by \tilde{b} .

prop:divbybexists

misp/ncb
Footnote.

For a tangle diagram D_T (representing a tangle T) and a crossing x of D_T , let $\epsilon(x) \in \{\pm 1\}$ be the sign of x , and $D_T|_{x \rightarrow \smile}$ be the diagram D_T with x replaced by a smoothing. We first define a map \check{b} from the free $\mathbb{C}[b]$ -module spanned by tangle diagrams, to $\tilde{\mathcal{T}}^1$, as the linear extension of the following:

$$\begin{aligned} b^k D_T &\xrightarrow{\check{b}} 0 \text{ if } k \geq 2, \\ b D_T &\xrightarrow{\check{b}} D_T, \\ D_T &\xrightarrow{\check{b}} \frac{1}{2} \sum_{x \text{ crossing of } T} \epsilon(x) D_T|_{x \rightarrow \smile}. \end{aligned}$$

We claim that this descends to a well defined map $\check{b} : \tilde{\mathcal{T}}_{\nabla}^{1/2} \rightarrow \tilde{\mathcal{T}}^1$. It is straightforward to check that the Reidemeister moves are in the kernel of \check{b} . We also need to verify that $\tilde{\mathcal{T}}_{\nabla}^2$ and the Conway relation are in the kernel.

An element of $\tilde{\mathcal{T}}_{\nabla}^2$ can be represented as a sum of terms $b^k D_T \in \tilde{\mathcal{T}}_{\nabla}^2$, where D_T is a tangle diagram with or without double points. If $k \geq 2$ then $\check{b}(b^k D_T) = 0$. If $k = 1$, then D_T has a double point, so $\check{b}(b D_T) = D_T$ is zero in $\tilde{\mathcal{T}}^1$. If $k = 0$, then D_T has at least two double points. Smoothing a crossing interferes with at most one of the double points, so $\check{b}(D_T)$ can be written as a sum of terms with at least one double point each. Hence $\check{b}(D_T) \in \tilde{\mathcal{T}}^1$ as well.

To show that the Conway relation vanishes, note that $\check{b}(\bowtie) = \check{b}(\nearrow - \nwarrow)$ is a sum with two types of terms: those which smooth a crossing that is a part of the double point, and those which smooth a crossing that is not. In the latter case, the double points are unchanged, so these terms are in $\tilde{\mathcal{T}}_{\nabla}^1$. From the terms where the crossings forming the double point are smoothed, we get

$$\check{b}(\bowtie - \nwarrow) = \frac{1}{2} \smile - (-1) \frac{1}{2} \smile = \smile = \check{b}(\smile),$$

as the Conway relation requires. Thus, \check{b} is well-defined on $\tilde{\mathcal{T}}_{\nabla}^{1/2}$.

Finally, \check{b} is clearly a one-sided inverse for \hat{b} , and therefore, \hat{b} is injective. \square

cor:divbyb

Corollary 4.20. *The map $\hat{b} : \tilde{\mathcal{T}}^1 \rightarrow \tilde{\mathcal{T}}_{\nabla}^{1/2}$ is a \mathbb{C} -linear isomorphism with inverse $\check{b} : \tilde{\mathcal{T}}_{\nabla}^{1/2} \rightarrow \tilde{\mathcal{T}}^1$.*

Notice that both \hat{b} and \check{b} shift the filtered degrees. The Goldman-bracket and Turaev cobracket are also degree-shifting, and these shifts will be realised by \hat{b} and \check{b} . The following fact in particular will be important in the construction of the Goldman bracket:

lem:mbOnCircle

Lemma 4.21. *The map \hat{b} restricts to an injective \mathbb{C} -linear map*

$$\hat{b} : \tilde{\mathcal{T}}^1(\bigcirc) \rightarrow \tilde{\mathcal{T}}_{\nabla}^{1/2}(\bigcirc\bigcirc).$$

Proof. Elements of $\tilde{\mathcal{T}}^1$ are linearly generated by the cosets of knots. Given a knot K , bK is equal in $\tilde{\mathcal{T}}^{1/2}$ to a difference of two two-component links, by a

single use of the Conway relation. Hence, the codomain is $\tilde{\mathcal{T}}^{1/2}(\bigcirc\bigcirc)$. Injectivity is inherited from \hat{b} on $\tilde{\mathcal{T}}^{1/1}$. \square

Note that this restriction of \hat{b} is not surjective to $\tilde{\mathcal{T}}^{1/2}(\bigcirc\bigcirc)$, for example, two-component links with a double point involving only one component are not in the image.

We introduce the same notation on the associated graded side:

def:Anot

Definition 4.22. $\tilde{\mathcal{A}}_{\nabla}$ is the quotient of $\tilde{\mathcal{A}}[[a]]$ by the chord diagram Conway relation. For a skeleton S , let $\tilde{\mathcal{A}}_{\nabla}(S)$ denote the image $\text{gr } \iota(\tilde{\mathcal{A}}(S))$. Also, let $\tilde{\mathcal{A}}^s := \tilde{\mathcal{A}} / \tilde{\mathcal{A}}^{\geq s}$ and $\tilde{\mathcal{A}}_{\nabla}^s := \tilde{\mathcal{A}}_{\nabla} / \tilde{\mathcal{A}}_{\nabla}^{\geq s}$.

By a straightforward calculation of the degree shifting associated graded maps we obtain:

rem:grdivbyb

Proposition 4.23. *The associated graded map of \hat{b} is an isomorphism $\text{gr } \hat{b} = \hat{a} : \tilde{\mathcal{A}}^1 \rightarrow \tilde{\mathcal{A}}^{1/2}$, which multiplies chord diagrams by a . The inverse is the isomorphism $\text{gr } \hat{b} = \check{a} : \tilde{\mathcal{A}}^{1/2} \rightarrow \tilde{\mathcal{A}}^1$. The isomorphism \check{a} divides by ‘ a ’ if a factor of ‘ a ’ is available; otherwise uses the Conway relation to smooth an s - s chord and obtain a factor of ‘ a ’ first. Furthermore, \hat{a} restricts to an injective map $\hat{a} : \tilde{\mathcal{A}}^1(\bigcirc) \rightarrow \tilde{\mathcal{A}}^{1/2}(\bigcirc\bigcirc)$. \square*

5. IDENTIFYING THE GOLDMAN-TURAEV LIE BIALGEBRA

In this section we establish our main results: we identify the Goldman-Turaev Lie bialgebra in the low s -filtered degree quotients of $\mathbb{C}\tilde{\mathcal{T}}$, and show that the Kontsevich integral induces a homomorphic expansion. The arguments follow the outline summarized in Section 2, and obtain the Goldman bracket and the self-intersection map μ as induced operations. In turn, the homomorphicity of the Kontsevich integral follows from the naturality of the construction.

5.1. The Goldman Bracket. Recall from Section 3.2 that D_p denotes the p -punctured disc, π is its fundamental group, and $|\mathbb{C}\pi|$ is the linear quotient $|\mathbb{C}\pi| := \mathbb{C}\pi / [\mathbb{C}\pi, \mathbb{C}\pi]$, which is linearly generated by homotopy classes of free loops in D_p . The Goldman bracket (Definition 3.2) is a lie bracket $[\cdot, \cdot]_G : |\mathbb{C}\pi| \otimes |\mathbb{C}\pi| \rightarrow |\mathbb{C}\pi|$. We start by identifying $|\mathbb{C}\pi|$ in a low degree quotient of $\mathbb{C}\tilde{\mathcal{T}}(\bigcirc)$ through a map β induced by the bottom projection.

prop:BotProj

Proposition 5.1. *The bottom projection $M_p \rightarrow D_p \times \{0\}$ induces a surjective filtered map*

$$\beta : \mathbb{C}\tilde{\mathcal{T}}_a(\bigcirc) \rightarrow |\mathbb{C}\pi|.$$

Proof. By the framed Reidemeister Theorem, framed knots in $\mathbb{C}\tilde{\mathcal{T}}(\bigcirc)$ are faithfully represented by knot diagrams in $D_p \times \{0\}$ – regular projections to the bottom with over/under information – modulo the framed Reidemeister moves (weak R1, R2, and R3). Diagrammatically, the bottom projection forgets the over/under

Do we need ∇ 's on the A's here? If not, then maybe we need a remark about why we dont.

check what happens with framed R1 when we mod out by the first step of the s -filtration...

IdentifyingGTinCON

identifybracketinCON

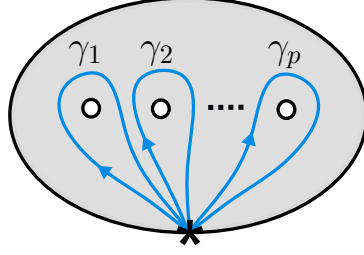
FIGURE 19. The standard generating curves of π .

fig:GenCurves

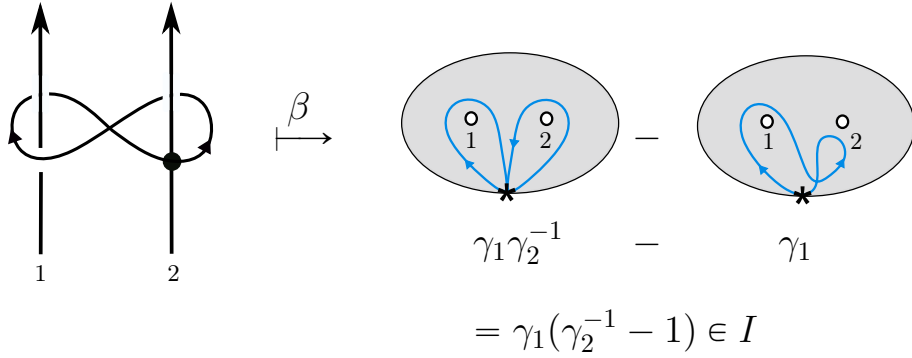
FIGURE 20. Example calculation demonstrating that β is a filtered map.

fig:BetaFiltered

information, in other words, imposes the relation $\nearrow = \nwarrow$. The images of the Reidemeister moves follow from the corresponding moves generating homotopies of immersed free loops, hence β is well-defined. The projection is clearly surjective as any loop can be lifted to a framed knot by introducing arbitrary under/over information at the crossings and imposing the blackboard framing.

The statement that β is filtered means that step k of the the Vassiliev t -filtration in $\mathbb{C}\tilde{\mathcal{T}}(\mathcal{O})$ projects to step k of the filtration on $|\mathbb{C}\pi|$ induced by the \mathbb{I} -adic filtration of π . Note that strand-strand double points and framing changes are in the kernel of β , thus, we only have something to prove for knots with k strand-pole double points.

Let $\gamma_1, \dots, \gamma_p$ denote the standard generators of π as in Figure 19. A knot $K \in \mathbb{C}\tilde{\mathcal{T}}(\mathcal{O})$ maps to a free loop in $|\mathbb{C}\pi|$, whose conjugacy class in π is represented as a word in the generators γ_i . A pole-strand double point on pole j maps to a difference between two curves passing on either side of the j 'th puncture (as in Figure 20). Therefore, one of the words in $\mathbb{C}\pi$ representing these curves can be obtained from the other by inserting a single letter $\gamma_j^{\pm 1}$. The double point, which represents the difference, thus maps to a product with a factor of $(\gamma_j^{\pm 1} - 1)$, and

a knot with k pole-strand double points maps to a product with k factors of the form $(\gamma_j^{\pm 1} - 1)$. This is by definition an element in \mathcal{I}^k . \square

prop:kerbeta

Proposition 5.2. *The kernel of β is $\tilde{\mathcal{T}}^1(\mathcal{O})$, and thus, β descends to a filtered linear isomorphism $\beta : \tilde{\mathcal{T}}^1(\mathcal{O}) \rightarrow |\mathbb{C}\pi|$.*

Proof. Two framed knots in $\mathbb{C}\tilde{\mathcal{T}}(\mathcal{O})$ project to the same loop in $|\mathbb{C}\pi|$ if and only if they differ by framing changes and (strand-strand) crossing changes, which generate exactly the step 1 of the s -filtration, that is, $\tilde{\mathcal{T}}^1(\mathcal{O})$. \square

Recall that $\tilde{\mathcal{A}}$ denotes the (degree completed) associated graded space of $\mathbb{C}\tilde{\mathcal{T}}$ with respect to the t -filtration. described as the space of admissible chord diagrams on a circle skeleton, as in Definition 4.6. The s -filtration on $\mathbb{C}\tilde{\mathcal{T}}$ induces a corresponding s -filtration on $\tilde{\mathcal{A}}$, and $\tilde{\mathcal{A}}^{\geq i}(\mathcal{O})$ denotes the i -th s -filtered component of $\tilde{\mathcal{A}}(\mathcal{O})$. We also denote $\tilde{\mathcal{A}}^i(\mathcal{O}) = \tilde{\mathcal{A}}(\mathcal{O}) / \tilde{\mathcal{A}}^{\geq i}(\mathcal{O})$.

Recall from Section 3.2 that the associated graded vector space of $|\mathbb{C}\pi|$ is $|\widehat{\text{FA}}|$, where $\text{FA} = \text{FA}\langle x_1, \dots, x_p \rangle$ denotes the free associative algebra over \mathbb{C} , and the linear quotient $|\widehat{\text{FA}}| = \text{FA} / [\text{FA}, \text{FA}]$ is the graded \mathbb{C} -vector space generated by cyclic words in the letters x_1, \dots, x_p . The graded Goldman bracket is a map $[-, -]_{\text{gr}G} : |\widehat{\text{FA}}| \otimes |\widehat{\text{FA}}| \rightarrow |\widehat{\text{FA}}|$, as defined in Proposition 3.6. Denote the degree completions of FA and $|\widehat{\text{FA}}|$ by $\widehat{\text{FA}}$ and $|\widehat{\widehat{\text{FA}}}|$. By applying the associated graded functor to β , we identify $|\widehat{\widehat{\text{FA}}}|$ as follows:

prop:gr_beta

Proposition 5.3. *The associated graded map $\text{gr } \beta : \tilde{\mathcal{A}}(\mathcal{O}) \rightarrow |\widehat{\widehat{\text{FA}}}|$ has kernel $\tilde{\mathcal{A}}^{\geq 1}(\mathcal{O})$. Hence, $\text{gr } \beta$ descends to an isomorphism $\text{gr } \beta : \tilde{\mathcal{A}}^1(\mathcal{O}) \rightarrow |\widehat{\widehat{\text{FA}}}|$.*

Proof. The statement follows from applying the associated graded functor to the filtered short exact sequence

$$0 \longrightarrow \tilde{\mathcal{T}}^1(\mathcal{O}) \longrightarrow \tilde{\mathcal{T}}(\mathcal{O}) \xrightarrow{\beta} |\mathbb{C}\pi| \longrightarrow 0.$$

The filtrations on $\tilde{\mathcal{T}}^1(\mathcal{O})$ and $|\mathbb{C}\pi|$ are induced from the filtration on $\tilde{\mathcal{T}}(\mathcal{O})$, as in Lemma 2.3, therefore the associated graded sequence is also exact. \square

rem:ChorsOnPoles

Remark 5.4. In $\tilde{\mathcal{A}}^1(\mathcal{O})$ chord diagrams with any strand-strand chords are zero. Thus, $\tilde{\mathcal{A}}^1(\mathcal{O})$ is spanned by chord diagrams on poles and a single circle strand, with strand-pole chords only: for an example see the left of Figure 21. Note also that all admissible 4T relations involve a strand-strand chord, and are zero in $\tilde{\mathcal{A}}^1$. This means that chord endings on the poles commute, and there are no further relations. Such a chord diagram corresponds naturally to a cyclic word by labeling the poles with x_1, \dots, x_p and reading along the circle skeleton, as on the right of Figure 21. Indeed, this is an isomorphism, and gives the explicit description of $\text{gr } \beta$.

Having identified the domain of the Goldman Bracket, $|\mathbb{C}\pi| \otimes |\mathbb{C}\pi|$, as $\tilde{\mathcal{T}}^1(\mathcal{O}) \otimes \tilde{\mathcal{T}}^1(\mathcal{O})$ through the identification β , we can now show that the Goldman bracket is induced – in the sense of Section 2 – by the stacking commutator on $\mathbb{C}\tilde{\mathcal{T}}$.

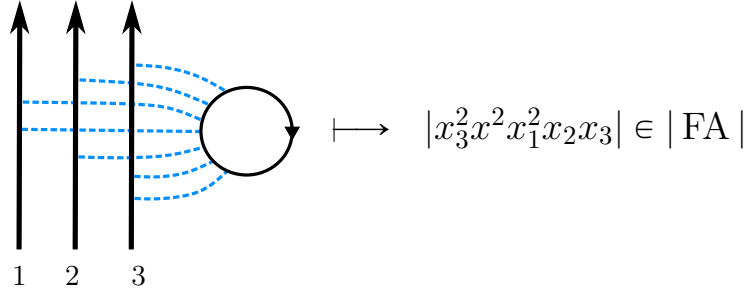


FIGURE 21. An example demonstrating how chord diagrams with no strand-strand chords can be read as cyclic words in $|FA|$.

fig:CycWord

$$\begin{array}{ccccccc}
 0 & \longrightarrow & \text{Ker} & \longrightarrow & \tilde{\mathcal{T}}_{\nabla}^{1/2}(\bigcirc) \otimes \tilde{\mathcal{T}}_{\nabla}^{1/2}(\bigcirc) & \longrightarrow & \tilde{\mathcal{T}}^{1/1}(\bigcirc) \otimes \tilde{\mathcal{T}}^{1/1}(\bigcirc) \longrightarrow 0 \\
 & & \downarrow 0 & & \downarrow \lambda & & \downarrow 0 \\
 0 & \longrightarrow & \tilde{\mathcal{T}}_{\nabla}^{1/2}(\bigcirc\bigcirc) & \longrightarrow & \tilde{\mathcal{T}}_{\nabla}^{1/2}(\bigcirc\bigcirc) & \longrightarrow & \tilde{\mathcal{T}}^{1/1}(\bigcirc\bigcirc) \longrightarrow 0 \\
 & & \uparrow \hat{b} & & \nwarrow \hat{\eta} & & \\
 & & \tilde{\mathcal{T}}^{1/1}(\bigcirc) & & & &
 \end{array}$$

η (curved arrow from $\tilde{\mathcal{T}}^{1/1}(\bigcirc)$ to $\tilde{\mathcal{T}}_{\nabla}^{1/2}(\bigcirc\bigcirc)$)
 $\hat{\eta}$ (curved arrow from $\tilde{\mathcal{T}}^{1/1}(\bigcirc\bigcirc)$ to $\tilde{\mathcal{T}}^{1/1}(\bigcirc)$)

FIGURE 22. Recovering the Goldman bracket. The horizontal maps are the natural quotient and inclusion maps, and Ker denotes the kernel of the consecutive projection. The map \hat{b} denotes multiplication by b (Lemma 4.21).

fig:Snakeforbracket

thm:bracketsnake

Theorem 5.5. Let $\lambda_1 : \tilde{\mathcal{T}}_{\nabla}^{1/2}(\bigcirc) \otimes \tilde{\mathcal{T}}_{\nabla}^{1/2}(\bigcirc) \rightarrow \tilde{\mathcal{T}}_{\nabla}^{1/2}(\bigcirc)$ denote the stacking product. Let λ_2 denote the opposite product given by $\lambda_2(K_1, K_2) = K_2 K_1$. The stacking commutator $\lambda = \lambda_1 - \lambda_2$ induces a unique map $\hat{\eta} : \tilde{\mathcal{T}}^{1/1}(\bigcirc) \otimes \tilde{\mathcal{T}}^{1/1}(\bigcirc) \rightarrow \tilde{\mathcal{T}}^{1/1}(\bigcirc)$, in the sense of the commutative diagram in Figure 22. The map $\hat{\eta}$ coincides with the Goldman bracket on $|\mathbb{C}\pi|$ via the identification $\beta : \tilde{\mathcal{T}}^{1/1}(\bigcirc) \xrightarrow{\cong} |\mathbb{C}\pi|$, that is,

$$[-, -]_G = \beta \circ \hat{\eta} \circ (\beta^{-1} \otimes \beta^{-1}).$$

Proof. The vector space $\tilde{\mathcal{T}}_{\nabla}^{1/2}(\bigcirc)$ is generated by the equivalence classes of knots in M_p . For $K_1, K_2 \in \tilde{\mathcal{T}}$, we abuse notation and denote by $K_1 \otimes K_2$ the class of $K_1 \otimes K_2$ in $\tilde{\mathcal{T}}_{\nabla}^{1/2}(\bigcirc) \otimes \tilde{\mathcal{T}}_{\nabla}^{1/2}(\bigcirc)$. The stacking commutator $\lambda(K_1 \otimes K_2) = K_1 K_2 - K_2 K_1$ is the difference between placing K_2 above or below K_1 in $D_p \times I$.

We first show that the right hand square of Figure 22 commutes. Regularly project K_1 , K_2 and their stacking products to the bottom D_p to obtain knot diagrams D_1 and D_2 , and link diagrams D_1D_2 and D_2D_1 . A *mixed crossing* of a link diagram be a crossing where the two strands belong to separate components. Notice that D_2D_1 is precisely D_1D_2 with all mixed crossings flipped.

Number the mixed crossings of D_1D_2 from 1 to r , and let L_i denote the link diagram where the first i mixed crossings have been flipped. Specifically, $L_0 = D_1D_2$ and $L_r = D_2D_1$. Then $L_0 - L_r = D_1D_2 - D_2D_1$ can be written as a telescopic sum:

eq:Telescope

$$(5.1) \quad D_1D_2 - D_2D_1 = (L_0 - L_1) + (L_1 - L_2) + \dots + (L_{r-1} - L_r).$$

In the sum, each term in parenthesis is a two-component link with a single mixed double point, with a sign (the crossing sign of the i -th mixed crossing). Thus, $\lambda(K_1, K_2) \in \tilde{\mathcal{T}}_{\nabla}^1$, and maps to zero in $\tilde{\mathcal{T}}_{\nabla}^1$. Hence, the right hand square commutes.

We now turn to the left square of the diagram. The kernel of the projection map

$$\tilde{\mathcal{T}}_{\nabla}^{1/2}(\mathbb{O}) \otimes \tilde{\mathcal{T}}_{\nabla}^{1/2}(\mathbb{O}) \rightarrow \tilde{\mathcal{T}}_{\nabla}^1(\mathbb{O}) \otimes \tilde{\mathcal{T}}_{\nabla}^1(\mathbb{O})$$

is generated by $\tilde{\mathcal{T}}_{\nabla}^{1/2}(\mathbb{O}) \otimes \tilde{\mathcal{T}}_{\nabla}^{1/2}(\mathbb{O})$ and $\tilde{\mathcal{T}}_{\nabla}^{1/2}(\mathbb{O}) \otimes \tilde{\mathcal{T}}_{\nabla}^{1/2}(\mathbb{O})$. Suppose that $K_1 \otimes K_2$ is in $\tilde{\mathcal{T}}_{\nabla}^{1/2}(\mathbb{O}) \otimes \tilde{\mathcal{T}}_{\nabla}^{1/2}(\mathbb{O})$; without loss of generality assume that K_1 is a knot with one double point. Then, by Equation 5.1, $\lambda(K_1 \otimes K_2)$ can be written as a telescopic sum of links with two double points each, hence it is zero in $\tilde{\mathcal{T}}_{\nabla}^{1/2}(\mathbb{O} \otimes \mathbb{O})$. Therefore, the left square commutes.

As in Section 2, then λ induces a unique map

$$\eta : \tilde{\mathcal{T}}^1(\mathbb{O}) \otimes \tilde{\mathcal{T}}^1(\mathbb{O}) \rightarrow \tilde{\mathcal{T}}_{\nabla}^{1/2}(\mathbb{O} \otimes \mathbb{O}).$$

We can now identify η as the Goldman bracket. The isomorphism β gives $\tilde{\mathcal{T}}^1(\mathbb{O}) \cong |\mathbb{C}\pi|$ (Proposition 5.2) identifies the domain of η with the domain of the Goldman bracket. We will argue that the image of η also lies in $\tilde{\mathcal{T}}^1(\mathbb{O}) \cong |\mathbb{C}\pi|$.

By Equation (5.1), $\lambda(K_1, K_2)$ can be written a sum of r terms, each with one mixed double point. Applying the Conway relation to each of the r terms of the telescopic sum by smoothing the mixed double points changes the skeletons from two circles to one circle, and introduces a factor of b :

eq:ConwayTel

$$(5.2) \quad \lambda(K_1 \otimes K_2) = D_1D_2 - D_2D_1 \stackrel{\nabla}{=} b(\epsilon_1 K_{s_1} + \epsilon_2 K_{s_2} + \dots + \epsilon_r K_{s_r}).$$

Here K_{s_i} denotes the knot obtained from $L_{i-1} - L_i$ by smoothing the mixed double point (which is obtained from the i -th mixed crossing), and ϵ_i is the sign of the i -th mixed crossing. That is, $\lambda(K_1, K_2) \in b\tilde{\mathcal{T}}_{\nabla}^{1/2}(\mathbb{O})$. In other words, η factors through $\tilde{\mathcal{T}}^1(\mathbb{O})$, which embeds in $\tilde{\mathcal{T}}_{\nabla}^{1/2}(\mathbb{O}, \mathbb{O})$ via the multiplication by b map \hat{b} , by Lemma 4.21. Hence, we obtain the map $\hat{\eta} : \tilde{\mathcal{T}}^1(\mathbb{O}) \otimes \tilde{\mathcal{T}}^1(\mathbb{O}) \rightarrow \tilde{\mathcal{T}}^1(\mathbb{O})$, as needed.

Finally, we check that $\hat{\eta}$ coincides with the Goldman bracket via the identification β . For curves $\gamma_1 \otimes \gamma_2 \in \tilde{\mathcal{T}}^1(\mathbb{O}) \otimes \tilde{\mathcal{T}}^1(\mathbb{O})$, let $K_1 \otimes K_2 \in \tilde{\mathcal{T}}_{\nabla}^{1/2}(\mathbb{O}) \otimes \tilde{\mathcal{T}}_{\nabla}^{1/2}(\mathbb{O})$

$$\begin{aligned}
& \text{Diagram 1} - \text{Diagram 2} = \text{Diagram 3} - \text{Diagram 4} \\
& \stackrel{\nabla}{=} b \left(\text{Diagram 5} - \text{Diagram 6} \right)
\end{aligned}$$

FIGURE 23. Example commutator bracket computation. The first equality is true after canceling terms in a telescoping expansion of the double points.

fig:combracket

$$\begin{array}{ccccccc}
0 & \longrightarrow & \text{Ker} & \longrightarrow & \tilde{\mathcal{A}}_{\nabla}^{1/2}(\mathcal{O}) \otimes \tilde{\mathcal{A}}_{\nabla}^{1/2}(\mathcal{O}) & \longrightarrow & \tilde{\mathcal{A}}_{\nabla}^{1/1}(\mathcal{O}) \otimes \tilde{\mathcal{A}}_{\nabla}^{1/1}(\mathcal{O}) \longrightarrow 0 \\
& & \downarrow 0 & & \downarrow \text{gr } \lambda & & \downarrow 0 \\
0 & \longrightarrow & \tilde{\mathcal{A}}_{\nabla}^{1/2}(\mathcal{O}\mathcal{O}) & \longrightarrow & \tilde{\mathcal{A}}_{\nabla}^{1/2}(\mathcal{O}\mathcal{O}) & \longrightarrow & \tilde{\mathcal{A}}_{\nabla}^{1/1}(\mathcal{O}\mathcal{O}) \longrightarrow 0 \\
& & \uparrow & & \uparrow \text{gr } \hat{\eta} & & \\
& & \tilde{\mathcal{A}}_{\nabla}^{1/1}(\mathcal{O}) & & & &
\end{array}$$

FIGURE 24. Recovering the graded Goldman bracket by applying the associated graded functor to the commutative diagram of Figure 22.

Snakefor_gr_bracket

be an arbitrary pre-image (vertical lift) of $\gamma_1 \otimes \gamma_2$. Then

$$\eta(\gamma_1 \otimes \gamma_2) = \frac{\lambda(K_1 \otimes K_2)}{b} \in \tilde{\mathcal{T}}^{1/1}(\mathcal{O}),$$

where we use the notation $\frac{1}{b}$ to mean composition with \check{b} . The Goldman bracket (Definition 3.2) is precisely a sum of smoothings of the mixed crossings of γ_1 and γ_2 . The only thing to check is that the crossing signs coincide with the negative signs of the local coordinate systems in the Goldman bracket definition, which is indeed the case. See Figure 23 for an example. \square

Recall that the graded Goldman bracket (Proposition 3.6) is a linear map $[-, -]_{\text{gr } G} : |\text{FA}| \otimes |\text{FA}| \rightarrow |\text{FA}|$, and by Proposition 5.3 we have an identification $\text{gr } \beta : |\text{FA}| \xrightarrow{\cong} \tilde{\mathcal{A}}^{1/1}(\mathcal{O})$. Applying the associated graded functor – with respect to the total filtration – to the diagram in Figure 22, we obtain the commutative diagram in Figure 24 and recover the graded Goldman bracket:

snakefor_gr_bracket

Corollary 5.6. *The diagram in Figure 24 commutes, the rows are exact, $\text{gr } \eta$ is the induced connecting homomorphism, and $\text{gr } \hat{\eta}$ agrees with the associated graded Goldman bracket via the identification $\text{gr } \beta : \tilde{\mathcal{A}}^1(\mathbb{O}) \xrightarrow{\cong} |\text{FA}|$. In other words,*

$$\text{gr}[\cdot, \cdot]_G = \text{gr } \beta \circ \text{gr } \hat{\eta} \circ (\text{gr } \beta^{-1} \otimes \text{gr } \beta^{-1}).$$

Proof. All arrows in the diagram in Figure 22 are filtered maps with respect to the total filtration; the rows are exact; and the total filtrations on the left and right hand sides are induced from the total filtration in the middle. Hence, Corollary 2.4 applies, and hence the gr functor gives a commutative diagram with exact rows, as in Figure 24. By the uniqueness of the connecting homomorphism, we know that it is $\text{gr } \eta$. By the functoriality of the associated graded, the graded Goldman bracket is given by

$$\text{gr}[\cdot, \cdot]_G = \text{gr } \beta \circ \text{gr } \hat{\eta} \circ (\text{gr } \beta^{-1} \otimes \text{gr } \beta^{-1}).$$

□

ex:grGoldman

Example 5.7. While the Corollary 5.6 follows from abstract considerations, let us demonstrate the on an example the explicit calculation of the graded bracket. Recall from Remark 5.4 that in $\tilde{\mathcal{A}}^1$ chord endings on the poles commute. The identification $\text{gr } \beta$ works by assigning a letter x_1, \dots, x_p to each pole, and reading off the cyclic word given by the chords along the circle skeleton component, as in Figure 21.

We compute the graded bracket of the words $|x_1 x_2^2|$ and $|x_2 x_3^2|$, via $\text{gr } \beta$. The two cyclic words correspond to chord diagrams in $\tilde{\mathcal{A}}^1(\mathbb{O})$, which we then consider in (lift to) $\tilde{\mathcal{A}}_{\nabla}^2(\mathbb{O})$. The map $\text{gr } \lambda$ is the stacking commutator of these diagrams, as shown in Figure 25. This lies in $\tilde{\mathcal{A}}_{\nabla}^{1/2}(\mathbb{O}\mathbb{O})$, which is easiest to see via applying a 4T relation for the letter coincidence x_2 , as shown in Figure 25. In turn, via an application of the Conway relation, it is easy to see that the element of $\tilde{\mathcal{A}}^1(\mathbb{O})$ which maps to this via multiplication by b is $|x_1^2 x_2 x_3^2| - |x_1^2 x_3^2 x_2|$. This is precisely the value of the graded Goldman bracket: compare also with Figure 6.

hm:Cube_for_bracket

Theorem 5.8. *The Kontsevich integral descends to a homomorphic expansion for the Goldman bracket, that is, the following diagram commutes:*

$$\begin{array}{ccc} |\mathbb{C}\pi| & \xleftarrow{[\cdot, \cdot]_G} & |\mathbb{C}\pi| \otimes |\mathbb{C}\pi| \\ \downarrow Z^1 & & \downarrow Z^1 \otimes Z^1 \\ |\widehat{\text{FA}}| & \xleftarrow{\text{gr}[\cdot, \cdot]_G} & |\widehat{\text{FA}}| \otimes |\widehat{\text{FA}}| \end{array}$$

Proof. The Kontsevich integral is homomorphic with respect to the stacking product (Proposition 4.10). Since λ , the key ingredient in our construction of $[\cdot, \cdot]_G$, is the difference between the stacking product and its opposite product, Z is

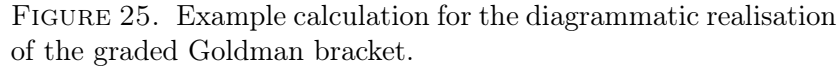


fig:GradedBracket

$$\begin{array}{ccc}
& \tilde{\mathcal{T}}_{\nabla}^{/2}(\mathcal{O}) \otimes \tilde{\mathcal{T}}_{\nabla}^{/2}(\mathcal{O}) & \\
\swarrow \lambda & & \downarrow Z^{/2} \otimes Z^{/2} \\
\tilde{\mathcal{T}}_{\nabla}^{/2}(\mathcal{O}\mathcal{O}) & & \tilde{\mathcal{A}}_{\nabla}^{/2}(\mathcal{O}) \otimes \tilde{\mathcal{A}}_{\nabla}^{/2}(\mathcal{O}) \\
\downarrow Z^{/2} & & \swarrow \text{gr } \lambda \\
\tilde{\mathcal{A}}_{\nabla}^{/2}(\mathcal{O}\mathcal{O}) & &
\end{array}$$
$$(5.3)$$

Hence, using the naturality of the induced map construction (Lemma 2.5 and the diagram (2.4)), we then know that the middle square of (5.4) commutes:

(5.4)

$$\begin{array}{ccc}
 \tilde{\mathcal{T}}^{1/1}(\mathcal{O}) & \xleftarrow{\hat{\eta}} & \tilde{\mathcal{T}}^{1/1}(\mathcal{O}) \otimes \tilde{\mathcal{T}}^{1/1}(\mathcal{O}) \\
 \downarrow & \xleftarrow{\eta} & \downarrow \\
 \tilde{\mathcal{T}}_{\nabla}^{1/2}(\mathcal{O}\mathcal{O}) & \xleftarrow{\eta} & \tilde{\mathcal{T}}^{1/1}(\mathcal{O}) \otimes \tilde{\mathcal{T}}^{1/1}(\mathcal{O}) \\
 \downarrow Z^{1/2} & & \downarrow Z^{1/1} \otimes Z^{1/1} \\
 \tilde{\mathcal{A}}_{\nabla}^{1/2}(\mathcal{O}\mathcal{O}) & \xleftarrow{\text{gr } \eta} & \tilde{\mathcal{A}}^{1/1}(\mathcal{O}) \otimes \tilde{\mathcal{A}}^{1/1}(\mathcal{O}) \\
 \uparrow & \xleftarrow{\text{gr } \hat{\eta}} & \uparrow \\
 \tilde{\mathcal{A}}^{1/1}(\mathcal{O}) & &
 \end{array}$$

(5.4)

Since all other faces of the diagram (5.4) are commutative by definition, the outside square also commutes. In turn, this is the middle square of the diagram (5.5):

$$\begin{array}{ccccccc}
 & & [\cdot, \cdot]_G & & & & \\
 & \swarrow & & \searrow & & & \\
 |\mathbb{C}\pi| & \xleftarrow[\beta]{\cong} & \tilde{\mathcal{T}}^{1/1}(\mathcal{O}) & \xleftarrow{\hat{\eta}} & \tilde{\mathcal{T}}^{1/1}(\mathcal{O}) \otimes \tilde{\mathcal{T}}^{1/1}(\mathcal{O}) & \xleftarrow[\beta^{-1} \otimes \beta^{-1}]{\cong} & |\mathbb{C}\pi| \otimes |\mathbb{C}\pi| \\
 \downarrow Z^{1/1} & & \downarrow Z^{1/1} & & \downarrow Z^{1/1} \otimes Z^{1/1} & & \downarrow Z^{1/1} \otimes Z^{1/1} \\
 |\widehat{\text{FA}}| & \xleftarrow[\text{gr } \beta]{\cong} & \tilde{\mathcal{A}}^{1/1}(\mathcal{O}) & \xleftarrow{\text{gr } \hat{\eta}} & \tilde{\mathcal{A}}^{1/1}(\mathcal{O}) \otimes \tilde{\mathcal{A}}^{1/1}(\mathcal{O}) & \xleftarrow[\text{gr } \beta^{-1} \otimes \text{gr } \beta^{-1}]{\cong} & |\widehat{\text{FA}}| \otimes |\widehat{\text{FA}}| \\
 & \swarrow & & \searrow & & & \\
 & & \text{gr}[\cdot, \cdot]_G & & & &
 \end{array}$$

Once again, all other faces of (5.5) are commutative: by Theorem 5.5 and Corollary 5.6 at the top and bottom; and otherwise by definition. Hence, the outside square commutes, and this is the statement of the theorem. \square

5.2. The Turaev co-bracket. In Section 3.2 we reviewed the definition of the Turaev cobracket on $|\mathbb{C}\pi|$ via the map $\mu : \mathbb{C}\tilde{\pi} \rightarrow |\mathbb{C}\pi| \otimes \mathbb{C}\pi$, which required choosing a rotation number $1/2$ representative for curves in $\mathbb{C}\tilde{\pi}$. The knot-theoretic version for the cobracket lifts this construction.

We start by interpreting $\mathbb{C}\tilde{\pi}$ in the context of tangles. Let interval denote an interval skeleton component where both endpoints are on the bottom $D_p \times \{0\}$. We call a tangle with skeleton \cap a **bottom tangle**. We mark the endpoints of the interval by \bullet and $*$, as in Figure 26. Furthermore, we denote by $\tilde{\mathcal{T}}(\mathcal{O}^k \cap^\ell)$ tangles with k circle skeleton components, and ℓ bottom intervals.

We extend the projection map β (Proposition 5.1) to such tangles to obtain an isomorphism similar to Corollary 5.1:

Proposition 5.9. *The natural bottom projection, post-composed with closing up open paths by concatenation with paths ν from the endpoint to the starting point along the boundary (as in Section 3.2) gives a filtered linear map*

$$\beta : \mathbb{C}\tilde{\mathcal{T}}_{\nabla}(\mathcal{O}^k \cap^\ell) \rightarrow |\mathbb{C}\pi|^{\otimes k} \otimes \mathbb{C}\pi^{\otimes \ell}$$

Inspired by [Hiro],

bring the figure next to.



has kernel $\tilde{\mathcal{T}}_{\nabla}^{\geq 1}(\bigcirc^k \cap^\ell)$, hence descends to a filtered isomorphism

$$\beta : \tilde{\mathcal{T}}^{1/1}(\bigcirc^k \cap^\ell) \xrightarrow{\cong} |\mathbb{C}\pi|^{\otimes k} \otimes \mathbb{C}\pi^{\otimes \ell}.$$

Proof. The proof is identical to the proof of Proposition 5.1, aside from the minor issue of base points. In the bottom projection, a tangle strand from \bullet to $*$ projects to a homotopy class of a path from \bullet to $*$ in D_p . Such paths are in bijection with $\mathbb{C}\pi$ via composition with a path ν along the boundary from $*$ to \bullet . \square

By straightforward inspection of the associated graded map, we obtain:

Proposition 5.10. *The associated graded map*

$$\text{gr } \beta : \tilde{\mathcal{A}}(\bigcirc^k \cap^\ell) \rightarrow |\text{FA}|^{\otimes k} \otimes \text{FA}^{\otimes \ell}$$

has kernel $\tilde{\mathcal{A}}^{\geq 1}(\cap)$, hence, $\text{gr } \beta$ descends to a graded isomorphism

$$\text{gr } \beta : \tilde{\mathcal{A}}^{1/1}(\bigcirc^k \cap^\ell) \xrightarrow{\cong} |\text{FA}|^{\otimes k} \otimes \text{FA}^{\otimes \ell}.$$

In particular, we have $\text{gr } \beta : \tilde{\mathcal{A}}^{1/1}(\cap) \xrightarrow{\cong} \text{FA}$.

We also extend the statements about multiplication and division by b to the context of mixed skeleta:

Proposition 5.11. *The map \hat{b} descends to \mathbb{C} -linear isomorphism*

$$\hat{b} : \tilde{\mathcal{T}}_{\nabla}^{1/1}(\bigcirc \cap) \xrightarrow{\cong} \tilde{\mathcal{T}}_{\nabla}^{1/2}(\cap),$$

with inverse map given by \check{b} , division by b .

Proof. From Corollary 4.20, we know \hat{b} is a \mathbb{C} -linear isomorphism $\tilde{\mathcal{T}}_{\nabla}^{1/1} \xrightarrow{\cong} \tilde{\mathcal{T}}_{\nabla}^{1/2}$, so we only need to address the change in skeleton. The quotient $\tilde{\mathcal{T}}_{\nabla}^{1/1}(\bigcirc \cap)$ is generated by classes of tangle diagrams D with skeleton consisting of one circle and one bottom-to-bottom interval component. After multiplication by b , $b \cdot D$ is equivalent via the Conway relation to a tangle with one double point in $\tilde{\mathcal{T}}(\cap)$, as the un-smoothing combines the two skeleton components. \square

Next, we recover the self intersection map μ , in the context of tangles, as the connecting homomorphism induced from the difference between two ways to lift a bottom tangle.

Let \bullet and $*$ be two “nearby” points on the boundary of D_p , that is, $*$ is obtained by shifting \bullet slightly forwards along the boundary orientation, as shown in Figure 26. We will obtain a homomorphic expansion for the Turaev cobracket by computing the Kontsevich integrals of one-strand tangles which start at \bullet and end at $*$. For this purpose, we will assume that \bullet and $*$ are *arbitrarily close*: technically, we take the limit of Kontsevich integrals as $*$ approaches \bullet backwards along the boundary. We suppress this in the notation, and write simply $Z(T)$ when we mean $\lim_{\bullet \leftarrow *} Z(T)$.

gr_beta_bot_tangle

p:qbonbottomtangles

$Z(T)$

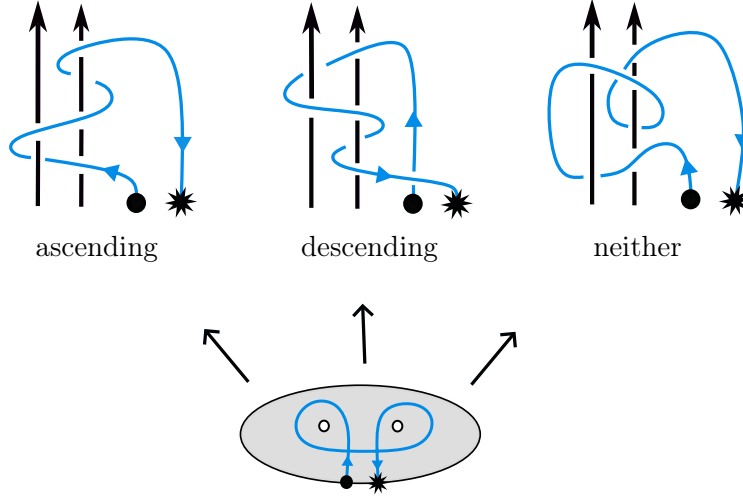


FIGURE 26. A curve in $\mathbb{C}\pi$ lifted to ascending, descending, and neither ascending nor descending bottom tangles. The three tangles are equivalent in $\tilde{\mathcal{T}}^{/1}$, but distinct in $\tilde{\mathcal{T}}$.

fig:ascending

def:asc+desc

Definition 5.12. An embedding

$$T : (I, \{0, 1\}) \hookrightarrow (M_p, \{\bullet, *\})$$

(representing a bottom tangle) is called *ascending* if it first ascends monotonically from \bullet , and then goes *straight* down to $*$. More precisely, if (z, s) is a global coordinate system for $M_p = D_p \times I$, then T is an ascending tangle if there exists $c \in (0, 1)$ such that when $t \in (0, c)$, the $\frac{d}{ds}$ component of \dot{T} is positive; when $t \in (c + \epsilon, 1)$, \dot{T} is a negative constant multiple of $\frac{d}{ds}$; and when $t \in (c, c + \epsilon)$, T smoothly transitions through a maximum.

Likewise, an embedding T is *descending* if it first goes straight up from \bullet , then monotonically descends to $*$. This can also be made precise as above. See Figure 26 for examples.

Definition 5.13. An *ascending tangle* is a bottom tangle in M_p whose ambient isotopy class has an ascending embedding. Similarly, a *descending tangle* is a bottom tangle in M_p whose ambient isotopy class has a descending embedding.

In the bottom projection, an ascending embedding will traverse each of its crossings on the under strand first, and on the over strand later. A descending embedding will traverse each crossing on the over strand first.

To recover μ , we need to define framed versions of the ascending and descending lifts. Given a curve γ in the fundamental group $\pi = \pi_1(D_p, *)$, γ has a unique lift $\tilde{\gamma}$ in $\tilde{\pi} = \tilde{\pi}_{\bullet,*}$ with the property that $\tilde{\gamma} \cdot \nu$ has rotation number zero, where

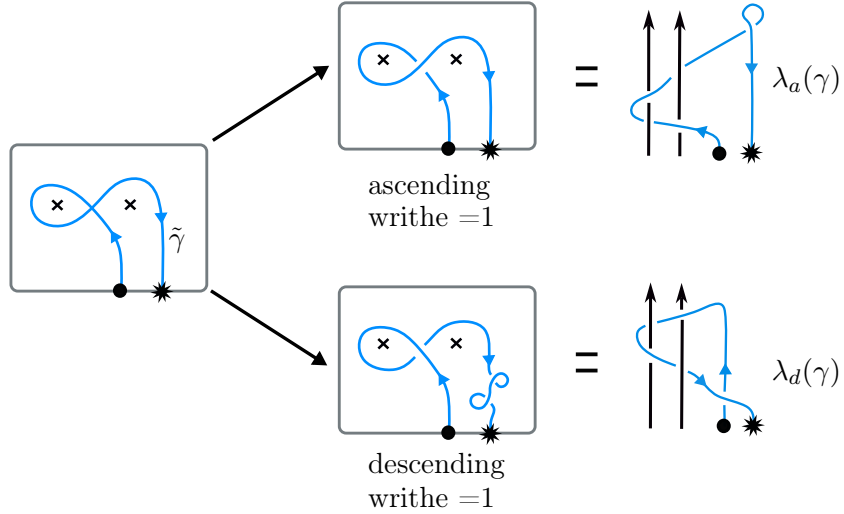


FIGURE 27. The framed ascending and descending lifts of a curve.

ν is a path along the boundary from $*$ to \bullet , as in Figure 3. Thus, the curve $\tilde{\gamma}$ lifts to a well-defined (up to isotopy) framed ascending tangle, where the framing is set to the blackboard framing. Denote this framed ascending lift by $\lambda_a(\gamma)$. To draw $\lambda_a(\gamma)$ in the bottom projection, one chooses the over and understands at every self intersection of γ so that each of the crossings are under-first: see Figure 27. Note that in this process punctures are irrelevant, and in the plane there is only one regular homotopy class of rotation number zero curves; therefore, the resulting framed tangle $\lambda_a(\gamma)$ will always have writhe 1 after connecting the endpoints along the boundary. When using different projection planes such as the back wall, one must take care to preserve the framed isotopy class of $\lambda_a(\gamma)$: in other words, we ensure that ascending lifts always have writhe 1. In the back projection, this means there is a small positive kink along the otherwise non-crossing ascending lift: see on the top right in Figure 27.

The natural descending lift of a rotation number 0 curve has writhe -1 , however, the difference of the lifts induces μ only if the framings agree. Hence, we set the writhe to $+1$ by convention. In the bottom projection, this manifests as two small positive “correction kinks” near the end of the curve, as in Figure 27. In the back wall projection, this is not needed, as shown in the bottom right of the same figure. We denote the framed descending lift of γ by $\lambda_d(\gamma)$.

Diagrammatically, in the bottom projection one obtains the descending lift from the ascending lift by changing all (strand-strand) crossings of the original curve, and one further crossing change for the framing correction, as shown in Figure 28.

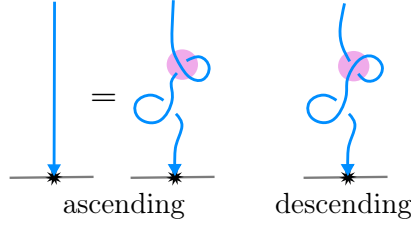


FIGURE 28. The framing correction of the descending lift is achieved by a single crossing change on the ascending lift, following a framed isotopy.

Via the isomorphism β , λ_a and λ_d can be seen as maps $\tilde{\mathcal{T}}^1(\cap) \rightarrow \tilde{\mathcal{T}}^2(\cap)$. Let $\bar{\lambda} : \tilde{\mathcal{T}}^1(\cap) \rightarrow \tilde{\mathcal{T}}^2(\cap)$ denote the difference

$$\bar{\lambda}(\gamma) = \lambda_a(\gamma) - \lambda_d(\gamma).$$

We are now ready to recover the self-intersection map $\mu : \mathbb{C}\pi \rightarrow |\mathbb{C}\pi| \otimes \mathbb{C}\pi$ (from Definition 3.3). Let q be the projection map from $\tilde{\mathcal{T}}_\nabla^{1/2}(\cap)$ to $\tilde{\mathcal{T}}^1(\cap)$

Theorem 5.14. *The map $\lambda = \bar{\lambda} \circ q$ induces a unique map*

$$\hat{\eta} : \tilde{\mathcal{T}}^1(\cap) \rightarrow \tilde{\mathcal{T}}^1(\bigcirc \cap)$$

in the sense of the commutative diagram of Figure 29. The map $\hat{\eta}$ agrees with the self-intersection map

$$\mu : \mathbb{C}\pi \rightarrow |\mathbb{C}\pi| \otimes \mathbb{C}\pi$$

under the identification $\beta : \tilde{\mathcal{T}}^1(\bigcirc^k \cap^\ell) \xrightarrow{\cong} |\mathbb{C}\pi|^{\otimes k} \otimes \mathbb{C}\pi^{\otimes \ell}$ up to a framing term. that is,

$$\mu = \beta \circ \hat{\eta} \circ \beta^{-1} + 1 \otimes \text{id},$$

where 1 denotes the constant loop.

Proof. We first show that the diagram of Figure 29 commutes. The commutativity of the left square is immediate from the exactness of the top row. The right side square is split into two triangles: of these the top one commutes by definition. The commutativity of the bottom triangle, that is, the fact that the post-composition of $\bar{\lambda}$ with the projection to $\tilde{\mathcal{T}}^1(\cap)$ is the zero map, is also straightforward, as follows. For a curve γ in $\tilde{\mathcal{T}}^1(\cap) \cong \mathbb{C}\pi$, the map $\bar{\lambda}$ is the difference of two lifts of γ to bottom tangles. When these lifts are subsequently projected back to $\tilde{\mathcal{T}}^1(\cap)$, they both project to γ , hence, their difference is 0.

Thus, as in Section 2, diagram (2.1), λ induces a unique well defined homomorphism $\eta : \tilde{\mathcal{T}}^1(\cap) \rightarrow \tilde{\mathcal{T}}_\nabla^{1/2}(\cap)$. By Proposition 5.11, the division by b map \check{b} restricts to an isomorphism $\check{b} : \tilde{\mathcal{T}}_\nabla^{1/2}(\cap) \rightarrow \tilde{\mathcal{T}}^1(\bigcirc \cap)$. The map $\hat{\eta} : \tilde{\mathcal{T}}^1(\cap) \rightarrow \tilde{\mathcal{T}}^1(\bigcirc \cap)$ is the composition $\hat{\eta} = \check{b} \circ \eta$.

$$\begin{array}{ccccccc}
& & \eta & & & & \\
& & \curvearrowright & & & & \\
\tilde{\mathcal{T}}_{\nabla}^{1/2}(\cap) & \longrightarrow & \tilde{\mathcal{T}}_{\nabla}^{1/2}(\cap) & \xrightarrow{q} & \tilde{\mathcal{T}}^1(\cap) & \longrightarrow & 0 \\
& \downarrow 0 & \downarrow \lambda = \bar{\lambda} \circ q & & \nwarrow \bar{\lambda} & \downarrow 0 & \\
0 \longrightarrow & \tilde{\mathcal{T}}_{\nabla}^{1/2}(\cap) & \longrightarrow & \tilde{\mathcal{T}}_{\nabla}^{1/2}(\cap) & \longrightarrow & \tilde{\mathcal{T}}^1(\cap) & \\
& \downarrow \check{b} & & & & & \\
& \tilde{\mathcal{T}}^1(\bigcirc \cap) & \xleftarrow{\hat{\eta}} & & & &
\end{array}$$

FIGURE 29. The nontrivial horizontal maps are the respective quotient maps, and q is one such quotient map.

fig:Snakeformu

It remains to show that $\mu = \beta \circ \hat{\eta} \circ \beta^{-1}$. Given a curve $\gamma \in |\mathbb{C}\pi|$, the value of $\beta \circ \hat{\eta} \circ \beta^{-1}$ is calculated as follows: γ is lifted to a curve of rotation number zero in $\tilde{\pi} = \tilde{\pi}_{\bullet,*}$, and, in turn, interpreted as an element in $\tilde{\mathcal{T}}^1(\cap)$. The map $\bar{\lambda}$ is applied to this framed curve, to obtain a difference of tangles in $\tilde{\mathcal{T}}_{\nabla}^{1/2}(\cap)$. This value is divided by b , and interpreted as a loop and a curve in $|\mathbb{C}\pi| \otimes \mathbb{C}\pi$.

Let γ be a curve in $\tilde{\mathcal{T}}^1(\cap) \cong \mathbb{C}\pi$, and let $\lambda_a(\gamma) = T_a$ be the framed ascending lift of γ and $\lambda_d(\gamma) = T_d$ the framed descending lift. Then $\bar{\lambda}(\gamma) = T_a - T_d$. Denote the bottom projection of T_a by D_a , and the bottom projection of T_d by D_d . In particular, D_d is obtained from D_a , by flipping all crossings arising from γ , and one of the crossings corresponding to the framing kinks.

As in the proof of Theorem 5.5, number the crossings to be flipped from 1 to r , with the framing kink being last. Let D_i denote the link diagram where the first i of the crossings have been flipped. Specifically, $D_0 = D_a$ and $D_r = D_d$. Then $D_0 - D_r$ can be written as a telescopic sum:

eq:Telescope2

$$(5.6) \quad D_0 - D_r = (D_0 - D_1) + (D_1 - D_2) + \dots + (D_{r-1} - D_r).$$

In the sum (5.6) each term $(D_i - D_{i+1})$ contains one (signed) double point corresponding to a self-intersection of γ . We apply the Conway relation ($\bowtie = b \cdot \wr$) at these double points. A straightforward check shows that the sign arising from the crossing signs of the first $(r-1)$ double points matches the sign $-\varepsilon_p$ in the definition of μ (Definition 3.3). The double point arising from the framing is $\bowtie - \wr = -\bowtie$ gives the framing term. Thus, dividing by b , reinterpreting via β , and adding $1 \otimes \gamma$ to cancel the framing term coincides with the value of $\mu(\gamma)$, as required. See Figure 30 for an example. \square

As with the Goldman bracket, the associated graded version of Theorem 5.14 follows:

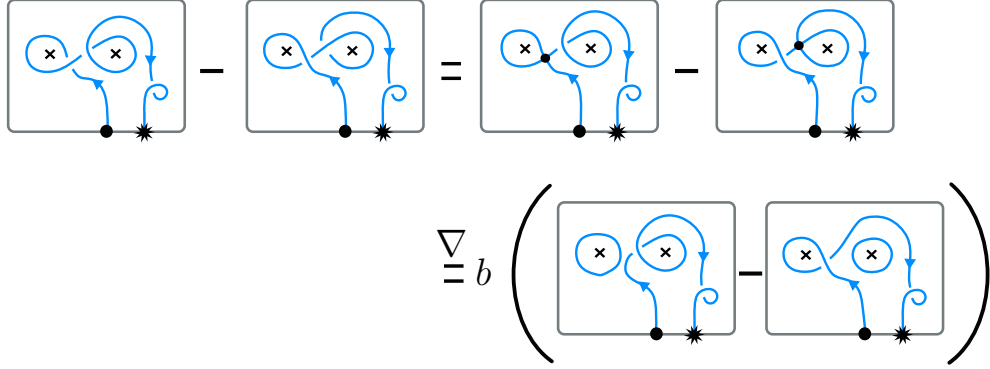


FIGURE 30. An example computation of the map $\hat{\eta}$: at the top left is the difference of the writhe 1 ascending and descending lifts of a curve. The latter is simplified as the negative kink cancels with one of the positive correction kinks.

fig:CobacketCalc

$$\begin{array}{ccccccc}
 & & \text{gr } \eta & & & & \\
 & & \curvearrowright & & & & \\
 \tilde{\mathcal{A}}_{\nabla}^{1/2}(\cap) & \longrightarrow & \tilde{\mathcal{A}}_{\nabla}^{2/2}(\cap) & \longrightarrow & \tilde{\mathcal{A}}_{\nabla}^{1/1}(\cap) & \longrightarrow & 0 \\
 \downarrow 0 & & \downarrow \text{gr } \lambda & & \downarrow 0 & & \\
 0 \longrightarrow & \tilde{\mathcal{A}}_{\nabla}^{1/2}(\cap) & \longrightarrow & \tilde{\mathcal{A}}_{\nabla}^{2/2}(\cap) & \longrightarrow & \tilde{\mathcal{A}}_{\nabla}^{1/1}(\cap) & \\
 \downarrow \text{gr } \check{b} & & & & & & \\
 \tilde{\mathcal{A}}^1(\bigcirc \cap) & \xleftarrow{\text{gr } \hat{\eta}} & & & & &
 \end{array}$$

FIGURE 31. Associated graded diagram constructing the graded self-intersection map.

akefor_gr_cobacket

cor:grmu

Corollary 5.15. *The diagram in Figure 31 commutes, the rows are exact, $\text{gr } \eta$ is the induced homomorphism, and $\text{gr } \mu = \text{gr } \beta \circ \text{gr } \hat{\eta} \circ (\text{gr } \beta)^{-1}$.*

Proof. The commutativity of the diagram (Figure 31) and the exactness of the rows follows from general principles in exactly the same way as Corollary 5.6. The rest is immediate, given that the framing term cancels in the associated graded map, as it is in filtered degree 0. \square

It is necessary for proving the formality statement – that is, the compatibility of the Kontsevich integral with the bracket and cobracket – to also have a concrete understanding of the associated graded map of λ . Recall from 5.4 and Proposition 5.10 that in $\tilde{\mathcal{A}}^1$ chord endings commute on the poles: this gives the isomorphism $\text{gr } \beta : \tilde{\mathcal{A}}^1(\cap) \rightarrow \text{FA}$.

Lemma 5.16. *Given a chord diagram $D \in \tilde{\mathcal{A}}^1(\cap)$, the map $\text{gr } \lambda_a : \tilde{\mathcal{A}}^1 \rightarrow \tilde{\mathcal{A}}_{\nabla}^{/2}$ orders the chord endings of D in an ascending order along the poles, that is, the ordering along the poles match the ordering along the strand. Similarly, $\text{gr } \lambda_d : \tilde{\mathcal{A}}^1 \rightarrow \tilde{\mathcal{A}}_{\nabla}^{/2}$ orders the chord endings of D along the poles in a descending order, that is, opposite to the ordering along the strand.*

Proof. This is immediate from the definition of the associated graded map, by choosing a singular tangle T_D representing D , and inspecting the chord diagram representing $\lambda_a(T_D)$ (respectively, $\lambda_d(T_D)$). \square

Recall from Section 3.2 that the Turaev cobracket $\delta : |\mathbb{C}\pi| \rightarrow |\mathbb{C}\pi| \otimes |\mathbb{C}\pi|$ is constructed from $\mu : \mathbb{C}\pi \rightarrow |\mathbb{C}\pi| \otimes \mathbb{C}\pi$ by post-composing μ with the trace map $\mathbb{C}\pi \rightarrow |\mathbb{C}\pi|$ in the second component, antisymmetrising (using $\text{Alt}(x \otimes y) = x \otimes y - y \otimes x$), and adding the framing term $|\gamma| \wedge 1$. The composition

$$\tilde{\delta} = \text{Alt} \circ (1 \otimes |\cdot|) \circ \mu + |\cdot| \wedge 1 : \mathbb{C}\pi \rightarrow |\mathbb{C}\pi| \otimes |\mathbb{C}\pi|$$

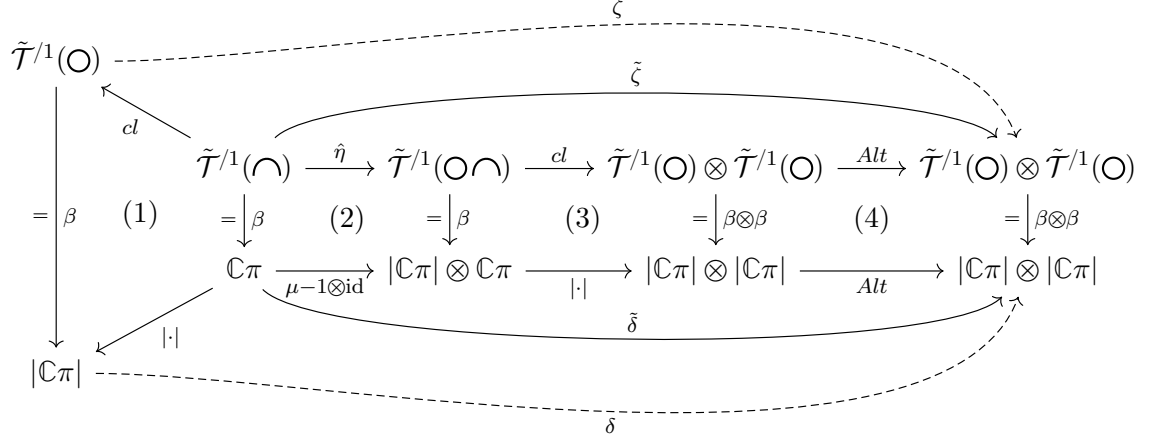
descends to the Turaev cobracket $\delta : |\mathbb{C}\pi| \rightarrow |\mathbb{C}\pi| \otimes |\mathbb{C}\pi|$, as in Definition 3.4.

We mimic this construction in the context of tangle diagrams by post-composing $\hat{\eta}$ with the closure map $\text{cl} : \tilde{\mathcal{T}}(\cap) \rightarrow \tilde{\mathcal{T}}(\bigcirc)$ on the open component, followed by anti-symmetrising, as shown in the diagram (5.7).

$$(5.7) \quad \begin{array}{ccc} \tilde{\mathcal{T}}^{/1}(\cap) & \xrightarrow{\hat{\eta}} & \tilde{\mathcal{T}}^{/1}(\bigcirc \cap) \\ & \searrow \hat{\zeta} & \downarrow \text{cl} \\ & & \tilde{\mathcal{T}}^{/1}(\bigcirc) \otimes \tilde{\mathcal{T}}^{/1}(\bigcirc) \\ & \searrow \tilde{\zeta} & \downarrow \text{Alt} \\ \tilde{\mathcal{T}}^{/1}(\bigcirc) & \xrightarrow{\zeta} & \tilde{\mathcal{T}}^{/1}(\bigcirc) \otimes \tilde{\mathcal{T}}^{/1}(\bigcirc) \end{array}$$

The closure map connects the endpoints of the bottom tangle, \bullet and $*$, by the path ν connecting $*$ to \bullet along the bottom boundary ∂D_p , following the orientation (as in Figure 3). We denote the map $\text{cl} \circ \hat{\eta} =: \hat{\zeta}$, and after antisymmetrisation $\text{Alt} \circ \hat{\zeta} =: \tilde{\zeta}$. We will show that $\tilde{\zeta}$ descends to a map $\zeta : \tilde{\mathcal{T}}^{/1}(\bigcirc) \rightarrow \tilde{\mathcal{T}}^{/1}(\bigcirc) \otimes \tilde{\mathcal{T}}^{/1}(\bigcirc)$, which realises the Turaev cobracket via the identification β . Since the framing correction term is already part of $\hat{\eta}$, it does not need to be added at this stage.

Proposition 5.17. *The map ζ realises the Turaev cobracket δ via the identifications β , in the sense that the diagram in Figure 32 commutes.*

FIGURE 32. The map ζ realises the Turaev cobracket δ .

Proof. The only substantial statement is the commutativity of the square (2): this is Theorem 5.14. Squares (1) and (3) are the same: the closure map corresponds to the trace $\mathbb{C}\pi \rightarrow |\mathbb{C}\pi|$. Square (4) is tautological. The maps $\tilde{\zeta}$ and $\tilde{\delta}$ are defined as the compositions shown: in the case of $\tilde{\delta}$ this is Definition 3.4. In particular, we have $\tilde{\delta} = (\beta \otimes \beta) \circ \tilde{\zeta} \circ \beta^{-1}$. The fact that $\tilde{\delta}$ descends to δ is Proposition 5.10 of [AKKN18b]. The fact that $\tilde{\zeta}$ descends to ζ is immediate from the canonical identifications. \square

Corollary 5.18. *The corresponding statement is true for the associated graded cobracket:*

$$\text{gr } \delta = (\text{gr } \beta \otimes \text{gr } \beta) \circ \text{gr } \zeta \circ \text{gr } \beta^{-1}.$$

\square

The key result left to prove is that ζ is homomorphic with respect to the Kontsevich integral Z : $\text{gr } \zeta \circ Z = Z \circ \zeta$, and hence the Kontsevich integral descends to a homomorphic expansion for δ . The subtlety involved is that Z does *not* respect the map $\hat{\eta}$ – there is an error term –, but after applying the closure, the error term cancels up to a framing correction, which subsequently cancels after alternation.

The proof is based on the naturality of the induced homomorphisms, as outlined in Section 2 and demonstrated in Section 5.1 for the Goldman bracket. The naive version of this idea would be to prove that all faces of a multi-cube similar to (5.3) commute. As before, the only non-trivial part of this statement is the commutativity of the middle square involving the map λ ; unfortunately, in the

case of the self-intersection map, this square fails to commute:

eq:FailToCommute

(5.8)

$$\begin{array}{ccc}
 & \tilde{\mathcal{T}}_{\nabla}^{/2}(\cap) & \\
 \swarrow \lambda & \downarrow Z^{/2} & \\
 \tilde{\mathcal{T}}_{\nabla}^{/2}(\cap) & \not\circlearrowleft & \tilde{\mathcal{A}}_{\nabla}^{/2}(\cap) \\
 \downarrow Z^{/2} & \swarrow \text{gr } \lambda & \\
 \tilde{\mathcal{A}}_{\nabla}^{/2}(\cap) & &
 \end{array}$$

This failure is mirrored in the setting of the Goldman–Turaev Lie bialgebra by the fact the the self-intersection map μ is *not formal*, only the Turaev cobracket obtained from it is [AKKN18b].

The resolution of this issue comes down to two observations:

- (1) The square (5.8) fails to commute by a controlled error; and
- (2) after applying the closure map and alternating to pass to the Turaev cobracket, this error vanishes.

In order to proceed we need to define an operation on $\tilde{\mathcal{T}}$, which will help relate the ascending and descending lifts. The *vertical flip*, or *flip* for short. This is a composition of a vertical mirror image (mirror image to the ceiling), with orientation reversal of each pole. In other words, the flip of a tangle is its vertical mirror image but with poles still ascending. The flip of a tangle T is denoted T^{\sharp} . The flip operation is also well-defined on the Conway quotient $\tilde{\mathcal{T}}_{\nabla}$ by setting $b^{\sharp} = -b$ for the variable b .

The associated graded *vertical flip*, or simply *flip*, of a chord diagram $D \in \tilde{\mathcal{A}}$, denoted D^{\sharp} , is the vertical mirror image of D with ascending poles, multiplied by $(-1)^s$, where s is the s -degree of D . This is because the mirror image reverses the signs of all crossings, then pole reversals reverse back the signs of all pole-strand crossings. Thus, only the signs of strand-strand crossings are reversed by the composite. On the Conway quotient $\tilde{\mathcal{A}}_{\nabla}$, the associated graded flip is given by setting $a^{\sharp} = -a$.

lem:CDflip

Lemma 5.19. *The Kontsevich integral respects flips:*

$$Z(T^{\sharp}) = (Z(T))^{\sharp}$$

for any $T \in \tilde{\mathcal{T}}$ or $T \in \tilde{\mathcal{T}}_{\nabla}$.

Proof. The Kontsevich integral is well known to respect mirror images and orientations switches, hence, it respects the composition. \square

The next lemma addresses the first of these steps by modifying the bottom arrow of (5.8) to correct the error:

lem:LambdaAlg

Lemma 5.20. *There exists a map $\lambda_a^{alg} : \tilde{\mathcal{A}}_{\nabla}^{/2}(\cap) \rightarrow \tilde{\mathcal{A}}_{\nabla}^{/2}(\cap)$ so that the diagram (5.10) commutes¹⁰.*

eq:FixedSquare

$$(5.9) \quad \begin{array}{ccc} \tilde{\mathcal{T}}_{\nabla}^{/2}(\cap) & \xleftarrow{\lambda} & \tilde{\mathcal{T}}_{\nabla}^{/2}(\cap) \\ Z^{/2} \downarrow & & \downarrow Z^{/2} \\ \tilde{\mathcal{A}}_{\nabla}^{/2}(\cap) & \xleftarrow{\lambda_a^{alg}} & \tilde{\mathcal{A}}_{\nabla}^{/2}(\cap) \end{array}$$

Proof. Recall that by definition, $\lambda = (\lambda_a - \lambda_d) \circ q$, where q is the projection $\tilde{\mathcal{T}}_{\nabla}^{/2}(\cap) \rightarrow \tilde{\mathcal{T}}^{/1}(\cap)$, and λ_a and λ_d are the ascending and descending lifts. Since the Kontsevich integral is compatible with the s -filtration and hence q , it is enough to show that the analogous statements are true for λ_a and λ_d separately. Namely, we show that there exist maps λ_a^{alg} and λ_d^{alg} making the following squares commute:

eq:FixedSquare

$$(5.10) \quad \begin{array}{ccc} \tilde{\mathcal{T}}_{\nabla}^{/2}(\cap) & \xleftarrow{\lambda_a} & \tilde{\mathcal{T}}^{/1}(\cap) \\ Z^{/2} \downarrow & & \downarrow Z^{/1} \\ \tilde{\mathcal{A}}_{\nabla}^{/2}(\cap) & \xleftarrow{\lambda_a^{alg}} & \tilde{\mathcal{A}}^{/1}(\cap) \end{array} \quad \begin{array}{ccc} \tilde{\mathcal{T}}_{\nabla}^{/2}(\cap) & \xleftarrow{\lambda_d} & \tilde{\mathcal{T}}^{/1}(\cap) \\ Z^{/2} \downarrow & & \downarrow Z^{/1} \\ \tilde{\mathcal{A}}_{\nabla}^{/2}(\cap) & \xleftarrow{\lambda_d^{alg}} & \tilde{\mathcal{A}}^{/1}(\cap) \end{array}$$

Let γ be a curve in $\tilde{\mathcal{T}}^{/1}(\cap)$. To find λ_a^{alg} , we need to express $Z^{/2}(\lambda_a(\gamma))$ in terms of $Z^{/1}(\gamma)$. Since the Kontsevich integral is compatible with the s -filtration, $Z^{/1}(\gamma) = Z^{/1}(\lambda_a(\gamma))$.

The proof thus depends on understanding the Kontsevich integral of $\lambda_a(\gamma)$: see Figure 33 for an expression of $\lambda_a(\gamma)$ as the tangle composition¹¹

eq:Asc

$$(5.11) \quad \lambda_a(\gamma) = \Phi^{-1} \beta \Phi RC.$$

Since the Kontsevich integral is multiplicative with respect to tangle composition,

eq:ZAsc

$$(5.12) \quad Z^{/2}(\lambda_a(\gamma)) = Z^{/2}(\Phi^{-1}) Z^{/2}(\beta) Z^{/2}(\Phi) Z^{/2}(R) Z^{/2}(C).$$

Since the Kontsevich integral asymptotically commutes with “distant disjoint unions” [CDM12, Chapter 8], the values of C , R and β include only chords in the highlighted areas of Figure 33. In particular, the value of the cap in C includes strand-strand chords only, and has no degree one term [BNGRT00], thus,

¹⁰Of course, $\lambda_a^{alg} \neq \text{gr } \lambda$.

¹¹We use notation inspired by Drinfel’d associators, but emphasise that these are classical Kontsevich integral calculations, not using the combinatorial construction in terms of the KZ associator. In particular, our definition of Z is in terms of limits (“infinitely near” and “infinitely far”), rather than parenthetisations.

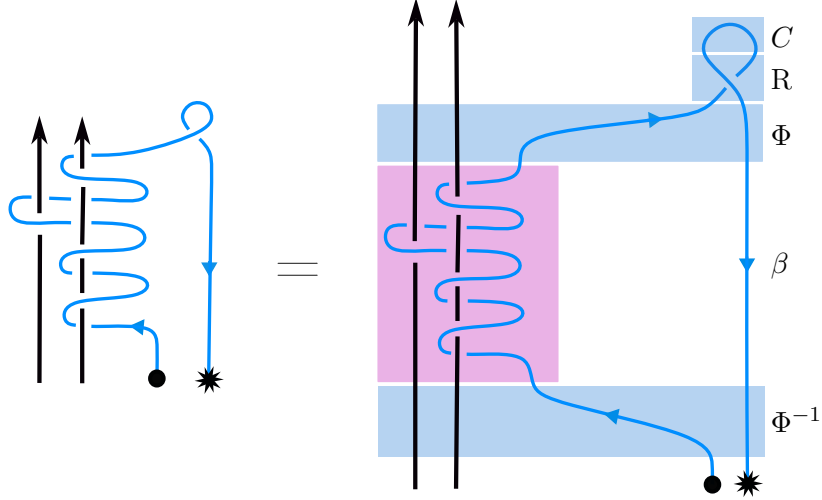
FIGURE 33. Tangle decomposition of the ascending lift $\lambda_a(\gamma)$.

fig:AscDecomp

$Z^{/2}(C) = 1$. The value $Z^{/2}(R)$ can be explicitly computed and is well known to be $1 + \frac{t}{2}$, where t denotes a single chord.

As for β , the value $Z^{/2}(\beta)$ has no strand-strand chords, and the strand-pole chords follow the strand in ascending order. Thus, by Lemma 5.16,

$$(5.13) \quad Z^{/2}(\beta) = \text{gr } \lambda_a(Z^{/1}(\gamma)).$$

eq:Zbeta

In summary, we have

$$(5.14) \quad Z^{/2}(\lambda_a(\gamma)) = Z^{/2}(\Phi^{-1}) \text{gr } \lambda_a(Z^{/1}(\gamma)) Z^{/2}(\Phi) \left(1 + \frac{t}{2}\right)$$

eq:ZAsc2

The formula can be further simplified by understanding $Z(\Phi_1)$. Since values of the Kontsevich integral are group-like, $Z(\Phi) = \exp(\varphi)$ for some primitive $\varphi \in \tilde{\mathcal{A}}(\uparrow\uparrow\downarrow)$. Since deleting either of the non-pole strands of $Z(\Phi)$ simplifies to 1, we have that $(Z(\Phi) - 1) \in \tilde{\mathcal{A}}^1$, and in particular $\varphi \in \tilde{\mathcal{A}}^1$. Thus,

$$(5.15) \quad Z^{/2}(\Phi) = 1 + \varphi \quad \text{with } \varphi \in \tilde{\mathcal{A}}^{1/2}$$

eq:ZPhi

Consequently, $Z^{/2}(\Phi^{-1}) = 1 - \varphi$. Substituting these values into (5.14), and expanding, we obtain

$$(5.16) \quad Z^{/2}(\lambda_a(\gamma)) = \text{gr } \lambda_a(Z^{/1}(\gamma)) + [\text{gr } \lambda_a(Z^{/1}(\gamma)), \varphi] + \text{gr } \lambda_a(Z^{/1}(\gamma)) \frac{t}{2},$$

eq:ZAsc3

where the square brackets denote the algebra commutator in $\tilde{\mathcal{A}}^{/2}(\uparrow\uparrow\downarrow)$.

In summary, for a diagram $D \in \tilde{\mathcal{A}}^{/1}(\cap)$, the map given by the formula

$$(5.17) \quad \lambda_a^{alg}(D) = \text{gr } \lambda_a(D) + [\text{gr } \lambda_a(D), \varphi] + \text{gr } \lambda_a(D) \frac{t}{2}$$

eq:AscAlg

completes the commutative diagram (5.10) for λ_a , as required. Note that φ does

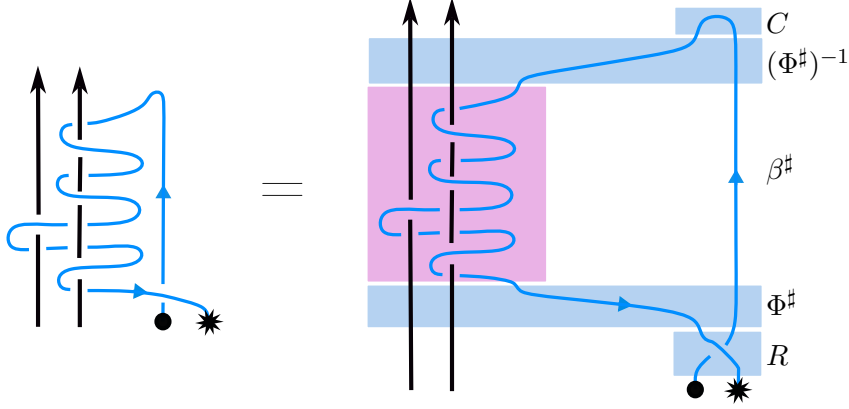
FIGURE 34. Tangle decomposition of the descending lift $\lambda_d(\gamma)$.

fig:DescDecomp

not depend on D .

Similarly for $\lambda_d(\gamma)$, Figure 34 shows that

$$(5.18) \quad Z^{1/2}(\lambda_d(\gamma)) = Z^{1/2}(R) \left(Z^{1/2}(\Phi^\sharp) Z^{1/2}(\beta^\sharp) Z^{1/2}(\Phi^\sharp)^{-1} \right)^{2,1},$$

eq:ZDesc

where β^\sharp and Φ^\sharp are the flip of β , and Φ , respectively, and the superscript “2, 1” indicates that the strands of these components are swapped.

Since $Z^{1/2}(\beta^\sharp)$ involves only strand-pole chords, and since the strand is descending, we have by Lemma 5.16:

$$(5.19) \quad Z^{1/2}(\beta^\sharp) = \text{gr } \lambda_d(Z^{1/1}(\gamma)).$$

eq:Zbeta

By Lemma 5.19 we have

$$(5.20) \quad Z^{1/2}(\Phi^\sharp) = (Z^{1/2}(\Phi))^\sharp = (1 + \varphi)^\sharp = 1 + \varphi^\sharp$$

eq:PhiSharp

In turn, $Z^{1/2}((\Phi^\sharp)^{-1}) = 1 - \varphi^\sharp$ and $Z^{1/2}(R) = (1 + \frac{t}{2})$. Substituting into (5.21), we obtain:

$$(5.21) \quad Z^{1/2}(\lambda_d(\gamma)) = \left(1 + \frac{t}{2} \right) \left((1 + \varphi^\sharp) \text{gr } \lambda_d(Z^{1/1}(\gamma)) (1 - \varphi^\sharp) \right)^{2,1}$$

eq:ZDesc

Expanded in $\tilde{\mathcal{A}}^{1/2}$, using that $t, \varphi \in \tilde{\mathcal{A}}^{1/2}$ this gives

$$(5.22) \quad Z^{1/2}(\lambda_d(\gamma)) = \text{gr } \lambda_d(Z^{1/1}(\gamma)) + \left[\varphi^\sharp, \text{gr } \lambda_d(Z^{1/1}(\gamma)) \right]^{2,1} + \frac{t}{2} \text{gr } \lambda_d(Z^{1/1}(\gamma))$$

eq:ZDesc2

Therefore, we define

$$(5.23) \quad \lambda_d^{alg}(D) = \text{gr } \lambda_d(D) + [\varphi^\sharp, \text{gr } \lambda_d(D)]^{2,1} + \frac{t}{2} \text{gr } \lambda_d(D)$$

eq:DescAlg

which completes the commutative diagram (5.10) for λ_d , as required.

$$\begin{array}{ccccccc}
& & & \eta^{alg} & & & \\
& & & \curvearrowright & & & \\
& \tilde{\mathcal{A}}_{\nabla}^{1/2}(\cap) & \longrightarrow & \tilde{\mathcal{A}}_{\nabla}^{2/2}(\cap) & \longrightarrow & \tilde{\mathcal{A}}_{\nabla}^{1/1}(\cap) & \longrightarrow 0 \\
& \downarrow 0 & & \downarrow \lambda^{alg} & & \downarrow 0 & \\
0 & \longrightarrow & \tilde{\mathcal{A}}_{\nabla}^{1/2}(\cap) & \longrightarrow & \tilde{\mathcal{A}}_{\nabla}^{2/2}(\cap) & \longrightarrow & \tilde{\mathcal{A}}_{\nabla}^{1/1}(\cap) \\
& \downarrow \text{gr } \check{b} & & & & & \\
& \tilde{\mathcal{A}}^1(\cap \cap) & \xleftarrow{\hat{\eta}^{alg}} & & & &
\end{array}$$

FIGURE 35. The diagram for the self-intersection map, with corrected associated graded maps.

Define $\bar{\lambda}^{alg} = \lambda_a^{alg} - \lambda_d^{alg}$, and $\lambda^{alg} = \bar{\lambda}^{alg} \circ q$, where q is the projection $\tilde{\mathcal{A}}_{\nabla}^{2/2} \rightarrow \tilde{\mathcal{A}}_{\nabla}^{1/1}$. Then, by definition, λ^{alg} makes the diagram (5.10) commute, completing the proof. \square

Since the formula for λ^{alg} will be important, we restate it as a proposition:

`prop:LambdaAlg`

Proposition 5.21. *The map λ^{alg} is defined by $\lambda^{alg} = (\lambda_a^{alg} - \lambda_d^{alg}) \circ q$, where*

$$\begin{aligned}
\lambda_a^{alg}(D) &= \text{gr } \lambda_a(D) + [\text{gr } \lambda_a(D), \varphi] + \text{gr } \lambda_a(D) \frac{t}{2} \\
\lambda_d^{alg}(D) &= \text{gr } \lambda_d(D) + [\varphi^\sharp, \text{gr } \lambda_d(D)]^{2,1} + \frac{t}{2} \text{gr } \lambda_d(D).
\end{aligned}$$

\square

`h:lambda_alg_diagram`

Lemma 5.22. *The map λ^{alg} fits into the commutative diagram of Figure 35 (solid arrows).*

Proof. The only non-empty part of this statement is that $q \circ \lambda^{alg} = 0$, that is, the composition of λ^{alg} with the projection to $\tilde{\mathcal{A}}_{\nabla}^{1/1}(\cap)$ is zero. We have seen before that this is true for $\text{gr } \lambda$, and it is shown in (5.17) and (5.23) that λ^{alg} differs from $\text{gr } \lambda$ in some correction terms. However, all of these correction terms are in s -degree 1 or higher (multiplicatively, 1 in s -degree 0), hence, $q \circ \lambda^{alg} = q \circ \text{gr } \lambda$. \square

We denote the induced map by $\hat{\eta}^{alg}$ and the composition of η^{alg} with $\text{gr } \check{b}$ by $\hat{\eta}^{alg}$, as shown in Figure 35.

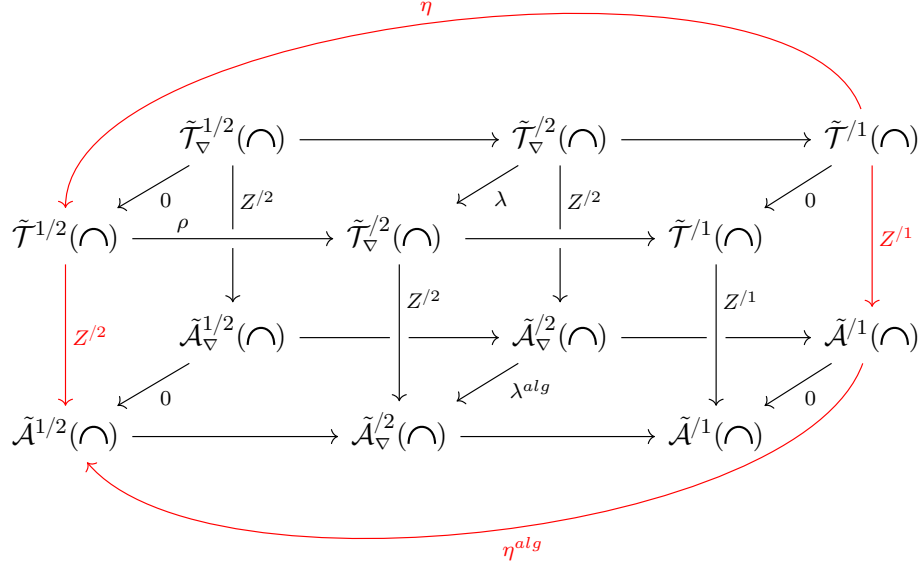


FIGURE 36. Commutative cube showing the compatibility of η and η^{alg} with the Kontsevich integral.

cor:Cube_for_cobacket

cor:ZEtaAlg

Corollary 5.23. *The Kontsevich integral is compatible with the map η and its corrected algebraic counterpart η^{alg} :*

$$(5.24) \quad \eta^{alg} \circ Z^1 = Z^2 \circ \eta,$$

and consequently,

$$(5.25) \quad \hat{\eta}^{alg} \circ Z^1 = Z^1 \circ \hat{\eta}.$$

Proof. If all faces of the multi-cube of Figure 36 commute, then this implies the statement, which itself is the commutativity of the diagonal (red) square. Indeed, all the faces of the multi-cube commute: the only non-trivial statement is the commutativity of the middle face, which was established in Lemma 5.20. Recall that $\hat{\eta}$ (respectively $\hat{\eta}^{alg}$) is obtained from η (respectively, η^{alg}) through division by b (respectively, division by a). Therefore, the second equality follows from the fact that the Kontsevich integral respects the s -filtration (Proposition 4.13). \square

We have now established that the square (5.8) commutes up to a controlled error: namely, it commutes if $\text{gr } \lambda$ is replaced by λ^{alg} , and furthermore, λ^{alg} is expressed explicitly in terms of $\text{gr}_a \lambda$ and $\text{gr } \lambda_d$ in Proposition 5.21 (and Equations (5.17) and (5.23)). In other words, we achieved the goal (1) stated above Lemma 5.20. Moving on to goal (2), we need to show that the error vanishes after

passing to the Turaev cobracket δ . Recall (Figure 32) that $\delta : |\mathbb{C}\pi| \rightarrow |\mathbb{C}\pi| \otimes |\mathbb{C}\pi|$, which descends from $\tilde{\delta} : \mathbb{C}\pi \rightarrow |\mathbb{C}\pi| \otimes |\mathbb{C}\pi|$. In turn, $\tilde{\delta} = \text{Alt} \circ (|\cdot| \otimes \text{id}) \circ \mu$ is identified via the isomorphisms β with the composition $\text{Alt} \circ \text{cl} \circ (\check{b} \circ \eta) = \text{Alt} \circ \text{cl} \circ \hat{\eta}$ by Theorem 5.14.

Theorem 5.24. *The Kontsevich integral descends to a homomorphic expansion for the ordered Turaev cobracket. Namely, $(Z^{/1} \otimes Z^{/1}) \circ \tilde{\delta} = \text{gr } \tilde{\delta} \circ Z^{/1}$, as shown in the diagram below, and consequently, $(Z^{/1} \otimes Z^{/1}) \circ \delta = \text{gr } \delta \circ Z^{/1}$.*

$$\begin{array}{ccccccc}
 & & & \tilde{\delta} & & & \\
 & \swarrow & & \searrow & & \swarrow & \\
 |\mathbb{C}\pi| \otimes |\mathbb{C}\pi| & \xleftarrow[\cong]{\beta \otimes \beta} & \tilde{\mathcal{T}}^{/1}(\bigcirc) \otimes \tilde{\mathcal{T}}^{/1}(\bigcirc) & \xleftarrow[\text{Alt} \circ \text{cl} \circ \check{\eta}]{} & \tilde{\mathcal{T}}^{/1}(\frown) & \xleftarrow[\cong]{\beta^{-1}} & \mathbb{C}\pi \\
 \downarrow Z^{/1} \otimes Z^{/1} & & \downarrow Z^{/1} \otimes Z^{/1} & & \downarrow Z^{/1} & & \downarrow Z^{/1} \\
 \widehat{\text{FA}} \otimes \widehat{\text{FA}} & \xleftarrow[\cong]{\text{gr } \beta \otimes \text{gr } \beta} & \mathcal{A}^{/1}(\bigcirc) \otimes \mathcal{A}^{/1}(\bigcirc) & \xleftarrow[\text{Alt} \circ \text{cl} \circ \text{gr } \hat{\eta}]{} & \mathcal{A}^{/1}(\frown) & \xleftarrow[\cong]{\text{gr } \beta^{-1}} & \widehat{\text{FA}} \\
 & \nwarrow & & \nearrow & & \nwarrow & \\
 & & & \text{gr } \hat{\delta} & & &
 \end{array}
 \tag{5.26}$$

Proof. If $\text{gr } \hat{\eta}$ were replaced with $\hat{\eta}^{alg}$ in the middle of the bottom row of (5.26), then this would be true by Corollary 5.23. Thus, it is enough to show that

$$\text{Alt} \circ \text{cl} \circ \hat{\eta}^{alg} = \text{Alt} \circ \text{cl} \circ \text{gr } \hat{\eta}.
 \tag{5.27}$$

Recall (from Figure 35) that

$$\hat{\eta}^{alg} = \text{gr } \check{\beta} \circ \left(\lambda_1^{alg} - \lambda_d^{alg} \right) = \frac{\lambda_a^{alg} - \lambda_d^{alg}}{a}.$$

Substituting the formulas of Proposition 5.21, we have

$$\begin{aligned}
 \hat{\eta}^{alg}(D) &= \frac{(\text{gr } \lambda_a - \text{gr } \lambda_d)(D)}{a} \\
 &\quad + \frac{[\text{gr } \lambda_a(D), \varphi] - [\varphi^\sharp, \text{gr } \lambda_d(D)]^{2,1} + \text{gr } \lambda_a(D) \frac{t}{2} - \frac{t}{2} \text{gr } \lambda_d(D)}{a}.
 \end{aligned}$$

By definition, we have that $\frac{(\text{gr } \lambda_a - \text{gr } \lambda_d)(D)}{a} = \text{gr } \hat{\eta}(D)$, hence, to prove (5.27) it is enough to show that the second line of the formula vanishes after closure and alternation. Namely, set

$$\begin{aligned}
 \varepsilon_1(D) &= \frac{[\text{gr } \lambda_a(D), \varphi] - [\varphi^\sharp, \text{gr } \lambda_d(D)]^{2,1}}{a}, \\
 \varepsilon_2(D) &= \frac{\text{gr } \lambda_a(D) \frac{t}{2} - \frac{t}{2} \text{gr } \lambda_d(D)}{a}.
 \end{aligned}$$

It is sufficient to prove that $Alt(cl(\varepsilon_1(D))) = 0$ and $Alt(cl(\varepsilon_2(D))) = 0$ for any $D \in \tilde{\mathcal{A}}^1(\cap)$.

For ε_1 , recall from the proof of Lemma 5.20 that $\varphi = Z^{1/2}(\Phi) - 1 \in \tilde{\mathcal{A}}^{1/2}$. The value φ is an infinite series graded by total degree; let X denote a term in φ . Since $X \in \tilde{\mathcal{A}}^{1/2}$, we can write $X = vtw$, as shown in Figure ?? . Here v and w are words in p letters (where p is the number of poles, and words are read in the direction of the strand), and t is the strand-strand chord.

By Lemma 5.19, the term corresponding to X in φ^\sharp is $X^\sharp = -wtv$, (see Figure ??). \square

sec:glossary

6. GLOSSARY OF NOTATION

a	formal variable of $\mathbb{C}\tilde{\mathcal{T}}_\nabla$	Def. 4.14	$\mathbb{C}\tilde{\mathcal{T}}$	formal linear combinations of
$\tilde{\mathcal{A}}$	associated graded $\mathbb{C}\tilde{\mathcal{T}}$	Sec. 4.3		oriented tangles in M_p
$\tilde{\mathcal{A}}_\nabla$	associated graded $\mathbb{C}\tilde{\mathcal{T}}_\nabla$,		$\mathbb{C}\tilde{\mathcal{T}}_\nabla$	Conway quotient of $\mathbb{C}\tilde{\mathcal{T}}$
	isomorphic to \mathcal{D}	Sec. 4.6	$\mathbb{C}\tilde{\mathcal{T}}_\nabla(S)$	the image $\iota(\mathbb{C}\tilde{\mathcal{T}}(S))$
$\tilde{\mathcal{A}}_\nabla(S)$	the image $\text{gr } \iota(\tilde{\mathcal{A}}(S))$	Def. 4.22	\bar{D}	vertical flip of diagram D
$\tilde{\mathcal{A}}_t$	degree t component of $\tilde{\mathcal{A}}$	Sec. 4.3	\mathcal{D}	$\sqcup_S \mathcal{D}(S)$
$\tilde{\mathcal{A}}^{\geq s}$	s -filtered component of $\tilde{\mathcal{A}}$		\mathcal{D}_∇	Conway quotient of \mathcal{D}
	$\tilde{\mathcal{A}}$	Def. 4.12	\mathcal{D}_t	$\sqcup_S \mathcal{D}_t(S)$
$\tilde{\mathcal{A}}(S)$	admissible chord diagrams on the skeleton S	Sec. 4.3	$\mathcal{D}(S)$	space of admissible chord diagrams on a skeleton S
$\tilde{\mathcal{A}}_{\nabla,t}$	degree t component of $\tilde{\mathcal{A}}_\nabla$	Sec. 4.6	$\mathcal{D}_t(S)$	degree t component of $\mathcal{D}(S)$
$\tilde{\mathcal{A}}_\nabla^s$	degree s component of $\tilde{\mathcal{A}}_\nabla$	Sec. 4.6	δ	Turaev Cobracket
$\tilde{\mathcal{A}}_{\nabla,t}^s$	$\tilde{\mathcal{A}}_{\nabla,t} \cap \tilde{\mathcal{A}}_\nabla^s$	Sec. 4.6	δ_{gr}	graded Turaev Cobracket
$\tilde{\mathcal{A}}^{/s}$	$\tilde{\mathcal{A}}/\tilde{\mathcal{A}}^{\geq s}$	Def. 4.22	$\tilde{\delta}$	$cl \circ \mu$
$\tilde{\mathcal{A}}_\nabla^{/s}$	$\tilde{\mathcal{A}}_\nabla/\tilde{\mathcal{A}}_\nabla^{\geq s}$	Def. 4.22	D_p	p -punctured disk
Alt	alternating map	Def. 3.4	$\eta, \hat{\eta}$	general notation for induced map from “ λ ”
b	$e^{\frac{a}{2}} - e^{-\frac{a}{2}}$	Def. 4.14		Thm. 5.5 and also Thm 5.14
\hat{b}	multiplication by b		$\eta^{alg}, \hat{\eta}^{alg}$	Fig. 35
\check{b}	map	Prop. 4.19	FA	degree completed free algebra
β	division by b map	Prop. 4.19		$\text{FA}\langle x_1, \dots, x_p \rangle$
\cap	bottom projection map	Prop. 5.1	$ \text{FA} $	$\text{FA}/[\text{FA}, \text{FA}]$
cl	bottom tangle	Sec. 5.2	$\widehat{\text{FA}}$	degree completion of FA
$\mathbb{C}\pi$	closure map	Sec. 5.2	$ \widehat{\text{FA}} $	degree completion of $ \text{FA} $
$ \mathbb{C}\pi $	group algebra of π	Sec. 3.2	$(-)^{\sharp}$	flip operation
	homotopy classes of free loops in D_p	Sec. 3.2	$[\cdot, \cdot]_G$	Goldman Bracket
$\mathbb{C}\tilde{\pi}$	group algebra of $\tilde{\pi}$	Sec. 3.2	$\text{gr } \mathbb{C}\pi$	graded $\mathbb{C}\pi$
$ \mathbb{C}\tilde{\pi} $	homotopy classes of immersed free loops in D_p	Sec. 3.2	$[\cdot, \cdot]_{\text{gr } G}$	graded Goldman Bracket
$ \overline{\mathbb{C}\pi} $	$ \mathbb{C}\pi /\mathbb{C}1$	Sec. 3.2	\mathcal{I}	augmentation ideal

ι		Sec. 4.6	q	general notation of a projection map	Thm. 5.14 and Lem 5.22
\mathcal{K}	links or tangles in \mathbb{R}^3	Sec. 3.1.1	$\tilde{\mathcal{T}}$	framed tangles in M_p	Def. 4.2
$\tilde{\mathcal{K}}$	framed links \mathbb{R}^3	Sec. 3.1.2	$\tilde{\mathcal{T}}^s$	s -filtered component of $\mathbb{C}\tilde{\mathcal{T}}$	Sec. 4.5
$\tilde{\mathcal{K}}_i$	filtered component of $\tilde{\mathcal{K}}$	Sec. 3.1.2	$\tilde{\mathcal{T}}_t^s$	$\tilde{\mathcal{T}}_t \cap \tilde{\mathcal{T}}^s$	Sec. 4.5
λ	general notation for a difference of two maps, $\lambda = \lambda_1 - \lambda_2$ in Thm. 5.5, $\lambda = (\lambda_a - \lambda_d) \circ q$ in Thm. 5.14		$\tilde{\mathcal{T}}_t$	t filtered component of $\mathbb{C}\tilde{\mathcal{T}}$	Sec. 4.3
λ_1, λ_2	stacking products	Thm. 5.5	$\tilde{\mathcal{T}}_\nabla^s$	s -filtered component of $\mathbb{C}\tilde{\mathcal{T}}_\nabla$	Sec. 4.6
λ_a	framed ascending lift	Sec. 5.2	$\tilde{\mathcal{T}}_{\nabla,t}$	t -filtered component of $\mathbb{C}\tilde{\mathcal{T}}_\nabla$	Sec. 4.6
λ_d	framed descending lift	Sec. 5.2	$\tilde{\mathcal{T}}_\nabla$	$\tilde{\mathcal{T}}/\tilde{\mathcal{T}}^n$	Sec. 4.6
$\bar{\lambda}$	$\lambda_a - \lambda_d$	Sec. 5.2	$\tilde{\mathcal{T}}^{1/n}$	$\mathbb{C}\tilde{\mathcal{T}}_\nabla/\tilde{\mathcal{T}}_\nabla^n$	Sec. 4.6
λ^{alg}		Lem. 5.20	$\tilde{\mathcal{T}}_\nabla^{1/n}$	$\tilde{\mathcal{T}}^1/\tilde{\mathcal{T}}^2$	Sec. 4.6
λ_a^{alg}		Eq. 5.17	$\tilde{\mathcal{T}}_\nabla^{1/2}$	$\tilde{\mathcal{T}}_\nabla^1/\tilde{\mathcal{T}}_\nabla^2$	Sec. 4.6
λ_d^{alg}		Eq. 5.23	$\tilde{\mathcal{T}}_\nabla^{1/2}$	$\tilde{\mathcal{T}}_\nabla^1/\tilde{\mathcal{T}}_\nabla^2$	Sec. 4.6
$\bar{\lambda}^{alg}$	$\lambda_a^{alg} - \lambda_d^{alg}$	Sec. 5.2	ξ	inward normal vector	Sec. 3.2
M_p	$D_p \times I$	Sec. 4.1	Z	Kontsevich Integral	
μ	self intersection map	Def. 3.3	Z_∇	Kontsevich Integral on $\mathbb{C}\tilde{\mathcal{T}}_\nabla$	Thm. 4.16
μ_{gr}	graded self intersection map	Prop. 3.7	$Z(T)$	Kontsevich Integral of one-stranded tangles	Sec. 5.2
ν	path from \star to \bullet	Sec. 3.2	ζ	map descending from $\tilde{\zeta}$	Sec. 5.2
ψ	chord contraction map	Lem. 4.7	$\tilde{\zeta}$	$Alt \circ \hat{\zeta}$	Sec. 5.2
π	$\pi_1(D_p, *)$	Sec. 3.2	$\hat{\zeta}$	$cl \circ \hat{\eta}$	Sec. 5.2
$\tilde{\pi}$	regular homotopy classes of immersed curves in D_p	Sec. 3.2	$\tilde{\zeta}$		

REFERENCES

- AKKN_highergen[AKKN18a] Anton Alekseev, Nariya Kawazumi, Yusuke Kuno, and Florian Naef. The goldman-turaev lie bialgebra and the kashiwara-vergne problem in higher genera, 2018.
- akkn_g0[AKKN18b] Anton Alekseev, Nariya Kawazumi, Yusuke Kuno, and Florian Naef. The goldman-turaev lie bialgebra in genus zero and the kashiwara-vergne problem. *Advances in Mathematics*, 326:1–53, 2018.
- AKKN_formality[AKKN20] Anton Alekseev, Nariya Kawazumi, Yusuke Kuno, and Florian Naef. Goldman-turaev formality implies kashiwara-vergne. *Quantum Topology*, 11(4):657–689, 2020.
- BN1[BN95] D. Bar-Natan. On the vassiliev knot invariants. *Topology*, 34:423–472, 1995.
- WK02[BND17] Dror Bar-Natan and Zsuzsanna Dancso. Finite type invariants of w-knotted objects II: tangles, foams and the Kashiwara-Vergne problem. *Math. Ann.*, 367(3-4):1517–1586, 2017.
- BN2[BNGRT00] Dror Bar-Natan, Stavros Garoufalidis, Lev Rozansky, and Dylan P. Thurston. Wheels, wheeling, and the kontsevich integral of the unknot. *Israel Journal of Mathematics*, 119:217–237, 2000.
- CDM_2012[CDM12] S. Chmutov, S. Duzhin, and J. Mostovoy. *Introduction to Vassiliev Knot Invariants*. Cambridge University Press, 2012.
- Da[Dan10] Zsuzsanna Dancso. On the kontsevich integral for knotted trivalent graphs. *Alg. Geom. Topol.*, 10(3):1317–1365, 2010.

- [Gol] [Gol86] William Mark Goldman. Invariant functions on lie groups and hamiltonian flows of surface group representations. *Invent. Math.*, 85:263–302, 1986.
- [Gor] [Gor99] Viktor Goryunov. Vassiliev invariants of knots in \mathbb{R}^3 and in a solid torus. *Differential and symplectic topology of knots and curves*, *Amer. Math. Soc. Transl.*, 190(2):37–59, 1999.
- [HM] [HM21] Kazuo Habiro and Gwénaél Massuyeau. The Kontsevich integral for bottom tangles in handlebodies. *Quantum Topol.*, 12(4):593–703, 2021.
- [Kon] [Kon93] Maxim Kontsevich. Vassiliev’s knot invariants. *Adv. in Soviet Math.*, 16(2):137–150, 1993.
- [Kuno25] [Kun25] Yusuke Kuno. Emergent version of drinfeld’s associator equations, 2025.
- [LM95] [LM95] Tu Quoc Thang Le and Jun Murakami. Kontsevich’s integral for the homfly polynomial and relations between values of multiple zeta functions. *Topology and its applications*, 62:193–206, 1995.
- [LM96] [LM96] Tu Quoc Thang Le and Jun Murakami. The universal Vassiliev-Kontsevich invariant for framed oriented links. *Compositio Mathematica*, 102(1):41–64, 1996.
- [Mag] [Mag35] W Magnus. Beziehungen zwischen gruppen und idealen in einem speziellen ring. *Mathematische Annalen*, 111:259–280, 1935.
- [Mas] [Mas18] Géwnael Massuyeau. Formal descriptions of turaev’s loop operations. *Quantum Topol.*, 9:39–117, 2018.
- [Tur] [Tur91] Vladimir Turaev. Skein quantization of poisson algebras of loops on surfaces. *Ann. Sci. École Norm. Sup.*, 24:635–704, 1991.

DEPARTMENT OF MATHEMATICS, UNIVERSITY OF TORONTO, TORONTO, ONTARIO, CANADA

Email address: drorbn@math.toronto.edu

URL: <http://www.math.toronto.edu/~drorbn>

SCHOOL OF MATHEMATICS AND STATISTICS, THE UNIVERSITY OF SYDNEY, SYDNEY, NSW, AUSTRALIA

Email address: zsuzsanna.dancso@sydney.edu.au

SCHOOL OF MATHEMATICS AND STATISTICS, THE UNIVERSITY OF MELBOURNE, MELBOURNE, VICTORIA, AUSTRALIA

Email address: hogant@student.unimelb.edu.au

URL: <https://www.tamaramaehogan.com/>

DEPARTMENT OF MATHEMATICS, UNIVERSITY OF TORONTO, TORONTO, ONTARIO, CANADA

Email address: chengjin.liu@mail.utoronto.ca

DEPARTMENT OF MATHEMATICS AND STATISTICS, ELON UNIVERSITY, ELON, NORTH CAROLINA

Email address: nscherich@elon.edu

URL: <http://www.nancyscherich.com>